ChemComm

FEATURE ARTICLE

View Article Online
View Journal | View Issue

Cite this: *Chem. Commun.*, 2026, **62**, 11014

Stimuli-responsive fluorogenic prodrugs of potent inhibitors targeting overexpressed metabolic enzymes in cancer

Pallavi Barman, Nikita Pal, † Rahul Kesarwani † and Krishna P. Bhabak *

Cancer cells are characterized by rapid, uncontrolled proliferation and rely on altered metabolic pathways to meet the heightened bioenergetic and biogenic demands required for tumour initiation, progression, and invasion. This metabolic reprogramming leads to the overexpression of specific metabolic enzymes that drive pathway-specific alterations to support tumour growth, survival and proliferation. For instance, cancer cells depend on aldose reductase (AR)-mediated glucose metabolism for proliferation, thymidylate synthase (TS)-mediated thymidylate biosynthesis and topoisomerase (Topo)-mediated DNA relaxation to facilitate faster DNA replication. Although specific inhibitors targeting many metabolic enzymes are widely used as chemotherapeutic agents/drugs, their clinical efficacy is often limited and compromised due to the lack of selectivity for cancer cells, poor pharmacokinetics, dose-related toxicities and the development of chemoresistance. Moreover, glutathione-*S*-transferases (GSTs), phase II metabolic enzymes frequently overexpressed in cancer cells, contribute to chemoresistance and thus represent an additional attractive therapeutic target. Recently, significant research efforts have been made towards developing various stimuli-responsive prodrugs that can selectively target enzymes overexpressed in cancer cells to enhance therapeutic efficacy. In this review, we highlight the importance of targeting four key metabolic enzymes from distinct metabolic pathways and discuss the recent developments of stimuli-responsive turn-on fluorogenic prodrugs of those specific enzyme inhibitors for achieving enhanced selectivity, improved anticancer efficacies and reduced off-target side effects, and for enabling real-time non-invasive monitoring of drug delivery with turn-on fluorescence read-out. The insights presented herein highlight the potential of stimuli-responsive fluorogenic prodrug strategies as a promising approach for modulating cancer metabolism and improving anticancer therapy.

Received 30th January 2026,
Accepted 20th May 2026

DOI: 10.1039/d6cc00654j

rsc.li/chemcomm

Department of Chemistry, Indian Institute of Technology Guwahati, Guwahati-781039, Assam, India. E-mail: kbhabak@iitg.ac.in
† Contributed equally to the work.

Pallavi Barman

Pallavi Barman earned her Integrated MSc in Chemistry from the National Institute of Technology Rourkela in 2020. She is currently a doctoral researcher at the Indian Institute of Technology Guwahati, working under the mentorship of Dr Krishna P. Bhabak. Her research focuses on the design and synthesis of organoselenium compounds and the mechanistic investigations of their anticancer activities in triple-negative breast cancer.

Nikita Pal

Nikita Pal received her BSc (2018) and MSc (2020) in Chemistry from the University of Calcutta, Kolkata. She is currently a Prime Minister's Research Fellow (PMRF) at the Indian Institute of Technology Guwahati, working under the supervision of Dr Krishna P. Bhabak. Her research focuses on the design and synthesis of biologically relevant organoselenocyanate conjugates and on the mechanistic investigation of their anticancer activities.

1. Introduction

Cancer cells, distinguished by rapid proliferation and the formation of expansive tumour masses, require ample energy and biomass to support their bioenergetics and biosynthetic activities, which are essential for macromolecule synthesis and cellular division. To surmount this proliferative constraint, cancer cells undergo extensive metabolic rewiring, a phenomenon now well-recognized as one of the hallmarks of cancer.[1] This metabolic reprogramming is an intricate process regulated by multiple signaling molecules, growth factors, proteins and enzymes that collectively remodel key cellular metabolic routes, including those modulating glucose, lipid, amino acid and nucleotide metabolism. Through these dysregulated and intertwined metabolisms, cancer cells sustain their anabolic and energetic needs, evade cell death and adapt to the hypoxic tumour microenvironment.[2,3]

Importantly, several critical metabolic enzymes are differentially overexpressed in cancer cells that drive pathway-specific alterations to fuel tumour growth, survival and proliferation (Fig. 1A). For instance, studies highlight the overexpression of key glycolytic enzymes, including Hexokinase II (HK-II) and Lactate Dehydrogenase A (LDHA), across a variety of cancer types.[4,5] This overexpression elevates glycolytic flux, thereby sustaining high glycolytic rates and contributing to the glycolytic phenotype of these cells.[6] Moreover, under hyperglycemic conditions, glucose is metabolized through the polyol pathway, where it is sequentially converted to fructose by Aldose Reductase (AR) and Sorbitol Dehydrogenase (SORD), ultimately promoting the invasive nature of cancer cells.[7,8] Above all, cancer cells rely heavily on fundamental building blocks, such as amino acids and nucleotides, to sustain an expedited rate of proliferation and cell division. Accumulating evidence suggests that amino acid levels are highly dysregulated in cancer cells to meet their increased nutrient demands while surviving in a nutrient-deprived microenvironment.[9] Moreover, amino acid metabolism influences not only protein synthesis in cancer cells but also nucleotide synthesis, signaling pathways, intracellular redox homeostasis and epigenetic modifications.[10] Notably, nucleotide metabolism is dysregulated in cancer cells to support the high rates of DNA replication and DNA repair mechanisms. This leads to the upregulation of specific enzymes involved in the biosynthesis of nucleotides through both *de novo* and salvage pathways (Fig. 1B). For instance, Ribonucleotide Reductase (RNR), Dihydrofolate Reductase (DHFR) and Thymidylate Synthase (TS) are overexpressed in a variety of organ-specific cancers to accelerate DNA synthesis in highly proliferating cells.[11] Furthermore, these proliferating cells undergo a robust DNA replication process, supported by key enzymes that meet the increased replicative demands (Fig. 1B). One such enzyme is Topoisomerase II (Topo-II), which introduces transient topological changes to the DNA macromolecule that facilitates DNA transcription and replication.[12] Collectively, these insights highlight that dysregulated metabolic enzymes are crucial drivers of cancer initiation and progression, making them potential targets of therapeutic intervention.

Although chemotherapy remains the primary treatment modality for cancer, chemotherapeutic drugs often encounter

Rahul Kesarwani

Rahul Kesarwani received his BSc (2017) and MSc (2019) degrees in chemistry from the University of Allahabad, Uttar Pradesh. Presently, he is pursuing doctoral research at the Indian Institute of Technology Guwahati under the guidance of Dr Krishna P. Bhabak. His research interests focus on the design and synthesis of fluorogenic prodrugs of important enzyme inhibitors and anticancer drugs for the effective treatment of cancer.

Krishna P. Bhabak

Krishna P. Bhabak received his BSc (2003) and MS (2006) in chemistry from Calcutta University and the Indian Institute of Science, Bangalore, respectively. He obtained his PhD (2009) from the Indian Institute of Science under the supervision of Prof. G. Mugesh. In 2010, he joined Humboldt-Universität zu Berlin as an Alexander von Humboldt Fellow to work with Prof. Christoph Arenz. After a short stay at the University of Oxford, UK, he joined Presidency University, Kolkata, as an Assistant Professor in 2013. He joined the Department of Chemistry, Indian Institute of Technology Guwahati, in 2015 as an Assistant Professor. Presently, he is an Associate Professor at the Indian Institute of Technology Guwahati. His research interests include the rational development of fluorogenic prodrugs of anticancer and anti-inflammatory drugs/agents. His research interests also include the development of organoselenium compounds as novel anticancer agents, with a focus on elucidating their mechanisms of action.

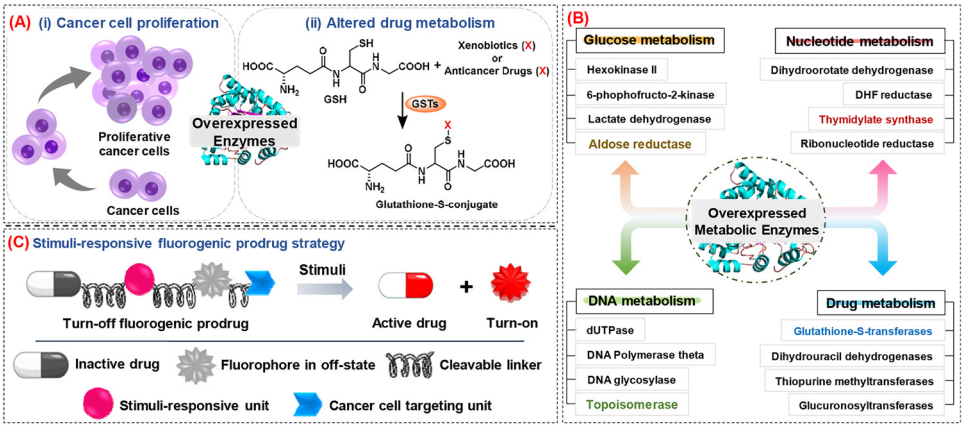

Fig. 1 (A) Overexpression of specific enzymes causes (i) cancer cell proliferation and (ii) altered drug metabolism. (B) Examples of a few overexpressed enzymes in cancer cells involved in glucose, DNA, nucleotide and drug metabolism. (C) Schematic representation of the stimuli-responsive turn-on fluorogenic prodrug model and its activation.

resistance in the treated cancer models due to several underlying mechanisms.[13] Growing evidence indicates that one important mechanism of resistance to chemotherapeutic agents is altered drug metabolism mediated by drug-metabolizing enzymes (DMEs), such as glutathione-*S*-transferases (GSTs), dihydropyrimidine (uracil) dehydrogenases (DPDs), uridine diphospho-glucuronosyltransferases (UGTs), and thiopurine methyltransferases (TPMTs) (Fig. 1B).[14] Notably, some chemotherapeutics depend on DMEs for their activation or deactivation. For example, irinotecan is activated by carboxylesterases and converted to the active metabolite SN-38,[13] whereas chlorambucil is detoxified to an inactive metabolite by GSTs *via* glutathione (GSH)-conjugation (Fig. 1A).[15] Importantly, GSTs are overexpressed in cancer cells, leading to enhanced phase II detoxification of electrophilic chemotherapeutic drugs, thereby contributing to increased chemoresistance. Therefore, recent research has focused on developing advanced therapeutic strategies that co-deliver chemotherapeutic drugs with GST inhibitors to overcome GST-mediated chemoresistance.[16,17] Consequently, GSTs have emerged as a promising therapeutic target for reducing chemoresistance in cancer patients with resistant tumours.

Interestingly, these classes of metabolic enzymes are druggable targets and are being exploited to develop and improve metabolic-targeted therapies for cancer treatment. Over the decades, several small-molecule inhibitors of key metabolic enzymes have entered preclinical and clinical evaluations as anticancer agents/drugs, as they have the potential to halt cancer cell proliferation, DNA replication, and division. For example, Lonidamine, an inhibitor of HK-II, has been explored as an anticancer agent either alone or in combination with other chemotherapeutic drugs, depending on the cancer type.[3] Moreover, 5-Fluorouracil (**5-FU**), an inhibitor of TS, and Doxorubicin, Daunorubicin and Etoposide, as inhibitors of Topo-II, are well-established anticancer drugs.[18,19] However, the clinical application of many such enzymatic inhibitors remains limited by their off-target side effects, poor selectivity, and inadequate biocompatibilities. To address these limitations, extensive efforts have been devoted to the development of stimuli-responsive turn-on fluorogenic prodrugs of metabolic enzyme inhibitors for effective cancer treatment (Fig. 1C). The small-molecule fluorogenic prodrug-based approach involves converting an active drug candidate into an ''inactive'' chemotherapeutic agent upon its conjugation with a specific stimulus-responsive unit and a fluorescent reporter *via* a cleavable non-toxic core or a self-immolative linker. Notably, the development of stimuli-responsive prodrugs for cancer treatment was facilitated by the prevalence of several dysregulated biological processes and parameters in the tumour microenvironment. For example, cancer cells or the tumour microenvironment is associated with a hypoxic milieu characterized by low pH, elevated levels of intracellular glutathione (GSH), hydrogen sulfide (H_2S), reactive oxygen species (ROS), and the overexpression of specific enzymes.[20] These features have been strategically exploited in the design of stimuli-responsive prodrugs, wherein specific functional moieties serve as stimuli-responsive units to activate the prodrugs (Fig. 1C). The stimuli-responsive turn-on fluorogenic prodrugs possess distinctive advantages over the conventional treatments with chemotherapy. Upon the reaction with cancer-specific biomarkers, the prodrug (i) releases the active drug at the targeted site, thereby eliciting an efficacious therapeutic outcome with reduced off-target side effects; (ii) enhances the bioavailability and biocompatibility of the active drug; (iii) simultaneously releases turn-on fluorogenic reporters, enabling a convenient, non-invasive and real-time monitoring of the drug delivery. Moreover, the targeting nature of the prodrug could be enhanced further by its conjugation with cancer cell-targeting ligands such as biotin, folate, galactose *etc.* (Fig. 1C). Notably, the self-immolative linkers in stimuli-responsive fluorogenic prodrugs play crucial roles in the drug uncaging process. For instance, it (i) leads to rapid and complete drug liberation, (ii) provides an amplification effect, where a single triggering event initiates a cascade reaction, enhancing efficiency and sensitivity, (iii) allows flexibility in responding to multiple stimuli and supports the development of advanced systems, including

theranostic prodrugs for real-time monitoring. Over the past decade, numerous studies have summarized the development of small-molecule stimuli-responsive fluorogenic prodrugs with reduced side effects and enhanced anticancer efficacy.[20–26] However, these reports have predominantly focused on the distinctive design strategies, stimuli-responsive behaviour and the choice of commercial chemotherapeutic drugs such as doxorubicin, cisplatin, paclitaxel, SN-38, **5-FU**, gemcitabine, *etc.*, with comparatively limited emphasis on their direct and specific molecular targets behind the selection of drugs. In this review, we primarily discuss the therapeutic relevance of targeting and inhibiting key metabolic enzymes such as AR, TS, Topo-II and GSTP1 in cancer mitigation. With a brief overview of reported inhibitors of these enzymes, we summarise the recent advances in the development of various stimuli-responsive fluorogenic prodrugs of the well-known inhibitors targeting these metabolic enzymes. We paid special attention to comprehensively discussing and critically analyzing the developmental strategies of the prodrugs over the last decade in achieving their optimal therapeutic activities while ameliorating off-target side effects to combat different organ-specific cancers.

2. Prodrugs of aldose reductase (AR) inhibitors

Recent findings highlight the differential expression of AR and its role in cancer cell metabolism under hyperglycemic conditions and oxidative stress-mediated inflammation, making it an important therapeutic target in cancer therapy.[27] While the enzyme was initially studied for its association with diabetic neuropathy and retinopathy, it is now being extensively investigated for its involvement in different organ-specific cancers, including hepatocellular carcinoma, breast cancer, lung cancer, cervical cancer and others.[28] AR is a member of the aldo-keto reductase (AKR) superfamily of proteins, with the AKR1B1 isoform playing a predominant role in the polyol pathway owing to its high affinity for glucose.[29] Under hyperglycemic conditions, approximately 30–50% of glucose is shunted through the polyol pathway, where overexpressed AR initiates its conversion to fructose *via* a two-step route. Mechanistically, AKR1B1 catalyzes the first and rate-limiting step of this pathway, reducing glucose to sorbitol using NADPH as a cofactor, followed by the oxidation of sorbitol to fructose by NAD^+-dependent sorbitol dehydrogenase (SD) (Fig. 2A). Consequently, the accumulation of sorbitol and fructose promotes cancer progression through multiple pathways. For instance, spontaneous alterations in the formation of these metabolites disrupt the homeostasis of the $NADPH/NADP^+$ and $NADH/NAD^+$ ratio, thus leading to increased oxidative stress and enhanced lactate dehydrogenase (LDH) activity, respectively.[27,30] In addition to this, AR has been reported to feed cancer cells by metabolizing the toxic lipid aldehydes to active metabolites useful for cellular proliferation (Fig. 2A). Furthermore, emerging evidence describes the involvement of overexpressed AR isoforms in the detoxification of chemotherapeutic drugs across a variety of organ-specific

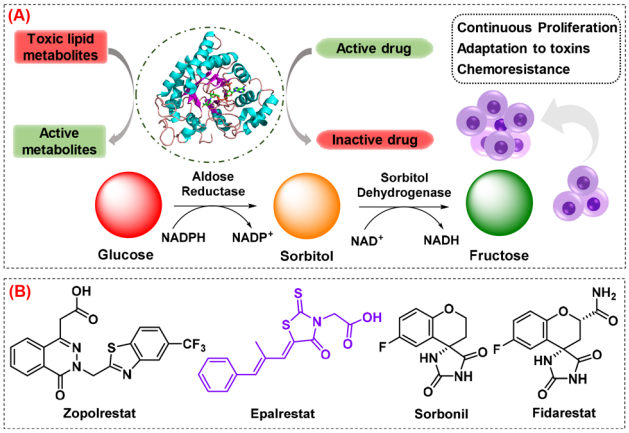

Fig. 2 (A) Catalytic pathways of AR and SD for the overall conversion of glucose to fructose as well as the detoxification of toxic lipids and inactivation of drugs. (B) Chemical structures of representative selective and potent inhibitors of AR.

cancers (Fig. 2A).[29] For example, AR contributes to resistance of doxorubicin in breast and colon cancer by reducing it to doxorubicinol, a largely inactive metabolite that is approximately one million-fold less potent against cancer cells while exhibiting pronounced cardiotoxicity.[31] Similarly, AR is shown to mediate resistance to cyclophosphamide, cisplatin and carboplatin in human medulloblastoma, ovarian, cervical, colon, and lung cancers.[32] Collectively, these findings emphasize the role of AR in cancer metabolism and prompt researchers to explore selective AR inhibitors as one of the potential therapeutic strategies in cancer treatment.

Over the past few decades, numerous AR inhibitors have been designed by considering the environment of the enzyme's catalytic site and have been reported to prevent diabetes-associated complications. These inhibitors are structurally classified into several groups, including acetic acid derivatives (tolrestat, epalrestat, ponalrestat, zopolrestat), spirohydantoin derivatives (sorbinil, fidarestat) and succinimide derivatives (AS-320) (Fig. 2B).[33] However, many of these inhibitors failed at different phases of clinical trials due to the requirement of a higher dose due to their off-target interactions, poor pharmacokinetic properties, and lack of specificity. Surprisingly, epalrestat (EPR) remains the only AKR1B1 inhibitor that is currently marketed in Japan, China and India for the treatment of human diabetic neuropathy.[34,35] Mechanistically, the central 2-thioxo-4-thiazolidinone group of EPR contributes to the inhibition of AKR1B1 by interacting with the indole –NH group of Trp111 within its catalytic site. This hydrogen-bonding interaction between EPR and the Trp111 residue induces conformational rearrangements in AKR1B1, thereby disrupting the NADPH-dependent conversion of glucose to sorbitol.[35,36] Nevertheless, EPR application in anticancer therapy is limited due to its highly hydrophobic nature and suboptimal pharmacokinetic properties. Therefore, significant research attention has been directed towards repurposing and structural remodelling of EPR for anticancer therapy, particularly through nanoformulation and prodrug-based strategies.[37,38]

In 2019, Mishra and co-workers developed a ratiometric redox-sensitive prodrug of EPR, co-loaded with doxorubicin (**Dox/EPR-SS-TPGS**) and investigated its synergistic effect on both *in vitro* (MDA-MB-231 and 4T1 cells) and *in vivo* (female BALB mice) models.[37] This strategy enhanced the sensitivity of MDA-MB-231 cells to doxorubicin, inducing prominent G2/M phase cell cycle arrest and significant apoptosis-mediated cell death with the downregulation of CD44 expression, implying the inhibition of cancer cell progression and invasion in metastatic states. Moreover, *in vivo* administration of **Dox/EPR-SS-TPGS-B6** resulted in significant inhibition of tumour growth while simultaneously alleviating Dox-mediated cardiotoxicity by downregulating troponin I, TNF-α, IL-6 and IL-1β. Collectively, these findings highlight the role of AR in conferring chemoresistance to the anticancer activity of Dox, and the problem could be overcome by the co-delivery of an AR inhibitor (EPR) with the anticancer drug (Dox).[37]

Surprisingly, the repurposing of EPR as a therapeutic agent for cancer treatment has not yet been adequately explored. Therefore, with the aim of reusing this drug for anticancer therapy, our group designed and developed an EPR prodrug to investigate the effects of the active drug with enhanced selectivity and improved bioavailability. In 2024, our group reported esterase-responsive, turn-on fluorogenic prodrugs of EPR, namely **RM-13** and **RM-28**, designed to selectively deliver the active drug to cancer cells with turn-on fluorescence by exploiting the overexpression of carboxylesterases in cancer cells.[38]

Notably, activation of the very weakly fluorescent prodrugs by porcine liver esterase (PLE) led to the deprotection of the 7-hydroxyl group of the coumarin unit, which subsequently activated the self-immolative process with the release of EPR (active drug) and the free fluorophore (**Cou-OH**) (Fig. 3A). Owing to the better hydrolytic stability of the pivaloyloxymethyl moiety in **RM-13**, the release of EPR in the presence of PLE was found to be slightly slower in comparison to **RM-28**, which contains a pivalate ester moiety as the esterase-responsive unit (Fig. 3B). The activation of prodrugs by PLE and the release of EPR was further monitored by reverse-phase HPLC analysis. While **RM-13** released 44.2% EPR, **RM-28** released 51.4% EPR after 12 h of incubation with PLE, indicating better esterase-responsive activation of **RM-28** over **RM-13** with turn-on fluorescence under physiological conditions. The PLE-induced uncaging of EPR from the prodrugs was further confirmed by

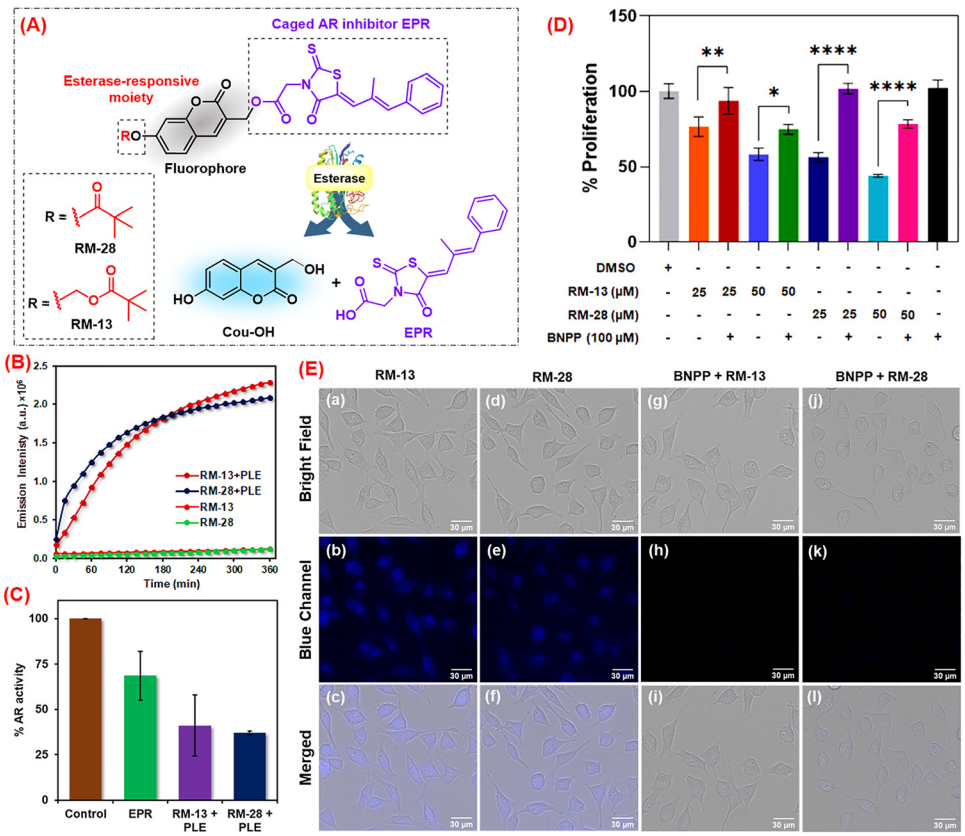

Fig. 3 (A) Chemical structures of the prodrugs (**RM-13** and **RM-28**) and their activation by esterases with the release of EPR and **Cou-OH**. (B) Emission spectra of **RM-13** (10 μM) and **RM-28** (10 μM) for 0–360 min in the absence and presence of PLE (0.5 U mL^{-1}). (C) Percentage AR activity upon treatment with **RM-13** (25 μM) + PLE (5.0 U mL^{-1}), **RM-28** (25 μM) + PLE (5.0 U mL^{-1}), and EPR (10 μM), along with the control AR activity. (D) Anti-proliferative activities of **RM-13** (25 and 50 μM) and **RM-28** (25 and 50 μM) in the presence/absence of BNPP (100 μM) against HeLa cells after 48 h. The quantitative data shown are mean ± SD (n = 3). *p < 0.05, **p < 0.01, and ****p < 0.0001. p values <0.05 were statistically significant based on one-way ANOVA. (E) Fluorescence microscopy images (bright field, blue channel, and merged) of HeLa cells in the presence of (a)–(c) **RM-13** (10 μM) and (d)–(f) **RM-28** (10 μM), and pre-treated with BNPP (500 μM; time, 3 h) followed by (g)–(i) **RM-13** (10 μM) and (j)–(l) **RM-28** (10 μM). The scale bar: 30 μm.

comparable inhibition of the recombinant AR by the prodrugs as well as free EPR (Fig. 3C).

The biocompatibility and the anticancer activity of the synthesized prodrugs was investigated in human cervical cancer (HeLa) cells. Interestingly, **RM-28** (IC_{50} ~ 50 μM) showed relatively higher potency than **RM-13**, which is consistent with the higher accessibility of **RM-28** towards cellular esterases. Moreover, the activation of prodrugs by the cellular esterases was further supported by the compromised anti-proliferative activities of both the prodrugs in the presence of known esterase inhibitor bis(4-nitrophenyl) phosphate (BNPP) (Fig. 3D).

The cellular uptake and the intracellular drug delivery were confirmed by the significantly increased fluorescence in the cells in the presence of **RM-13** and **RM-28**, which were activated by the endogenous esterases with the release of free fluorophore **Cou-OH** (Fig. 3E). This work thus suggests the importance of functionalizing the free carboxylic acid group of EPR, which may otherwise act as a barrier to cellular uptake. Moreover, prodrugs exert their anticancer activity in HeLa cells by arresting the cell cycle progression at the G2/M phase, similar to free EPR, thereby validating the potency of the prodrugs through the release of EPR under *in vitro* conditions. Taken together, these results highlight the use of endogenous stimuli to help release EPR at the targeted site with real-time non-invasive monitoring, enhanced bioavailability and potent anticancer activity.[38]

Additionally, other AKR1B1 inhibitors such as Zopolrestat and Fidarestat are being investigated for their anticancer activity and chemosensitizing potential; however, prodrug-based strategies are needed to mitigate off-target toxicities and enhance clinical efficacy.[31,39,40]

3. Prodrugs of thymidylate synthase (TS) inhibitors

During DNA replication, cancer cells rely heavily on *de novo* nucleotide synthesis and consequently reprogram their nucleotide metabolism through the upregulation of key enzymes, such as dihydroorotate dehydrogenase (DHODH), RNR, DHFR and TS.[11] Particularly, TS is involved in the biosynthesis of thymidylate, an essential precursor of DNA synthesis. Mechanistically, the catalytic site of TS binds the 2′-deoxyuridine 5-monophosphate (dUMP) and the co-factor CH_2THF (5,10-methylenetetrahydrofolate) to form a ternary complex. This complex catalyzes the reductive methylation of dUMP using CH_2THF as a methyl group donor, generating deoxythymidine-5′-monophoshate (dTMP) (Fig. 4A).[41] The resulting dTMP is subsequently phosphorylated to the triphosphate state (dTTP), which serves as a direct precursor of DNA synthesis. Importantly, TS is known as the only enzyme responsible for the *de novo* synthesis of thymine nucleotide precursors, making it a crucial enzyme in DNA replication and repair.[41] Several published reports indicate that this rate-limiting enzyme is overexpressed in highly proliferating cancer cells, including breast, colon, lung, gastric and pancreatic cancers.[42] Thus, the overexpression of TS in cancer cells fuels the increased production of DNA building blocks, thereby

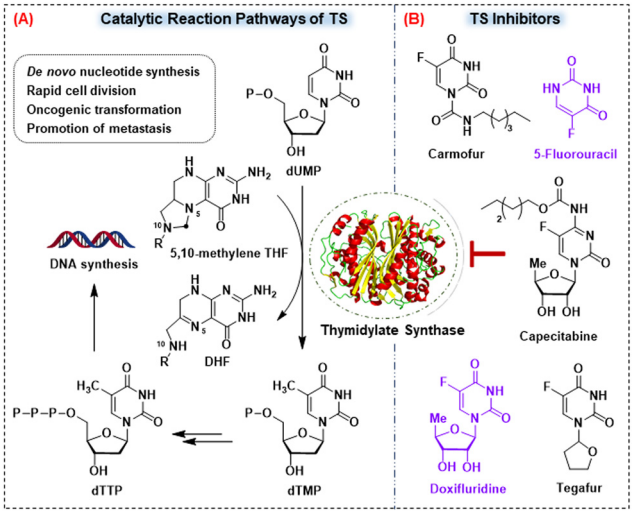

Fig. 4 (A) The catalytic pathways of TS for the conversion of dUMP to dTMP and its subsequent phosphorylation towards DNA synthesis and (B) Chemical structures of some representative inhibitors of TS.

supporting faster DNA replication and rapid cell division. Therefore, the involvement of TS in cancer development makes it an important prognostic biomarker and a critical target for cancer therapeutics. Over the decades, several efforts have been directed towards the structure-guided development of TS inhibitors, including fluoropyrimidine and folate derivatives, targeting the substrate-binding sites essential for TS activity (Fig. 4B).[43]

5-FU was the first fluoropyrimidine class of TS inhibitor to exhibit anticancer effects in clinical levels.[44] It exerts its effect through its active metabolite, fluorodeoxyuridine monophosphate (FdUMP), which forms a stable ternary complex with TS and CH_2THF, thereby irreversibly inhibiting TS activity. This inhibition prevents the conversion of dUMP to dTMP, which is necessary for DNA replication. Moreover, this leads to increased incorporation of fluorodeoxyuridine triphosphate (FdUTP) and fluorouridine triphosphate (FUTP) into DNA and RNA structures, respectively, resulting in DNA damage and disrupted protein translation.[45] Although **5-FU** is used as the first-line treatment and adjuvant chemotherapy for various organ-specific cancers, such as breast, colon, and lung, its clinical application is limited due to several drawbacks, including short half-life (10–20 min) and off-target toxicity.[46] Furthermore, alterations in the expression levels of enzymes involved in the metabolism of **5-FU** play a critical role in reducing its sensitivity to colorectal cancer. Therefore, to overcome the poor pharmacokinetic stability of **5-FU**, several studies have reported the development of mutual prodrugs and small-molecule prodrugs of **5-FU**, among which tegafur, doxifluridine, carmofur, and capecitabine are widely used clinically (Fig. 4B).[46,47] Despite this progress, small-molecule **5-FU** prodrugs lacking cancer cell-specific directing units still suffer from significant off-target toxicities, thereby limiting their clinical utility. With this in mind, researchers have focused on developing advanced stimuli-responsive prodrugs of **5-FU** by anchoring the tumour microenvironment-responsive moieties

to enhance selectivity towards cancer cells and improve pharmacokinetic stability.[48,49]

Over the last decade, researchers have significantly focused on the development of stimuli-responsive, turn-on fluorogenic prodrugs of TS inhibitors to enable real-time bio-imaging and *in situ* monitoring of drug accumulation, while simultaneously reducing systemic toxicity, and drug resistance. In 2014, Kim and co-workers reported the first biotin-anchored mitochondria-targeting ROS-responsive theranostic prodrug of doxifluridine, which exhibited selective toxicity against lung cancer (A549) cells over normal lung cells (WI38) by inducing intrinsic apoptosis.[50] The authors report that the prodrug localizes in the mitochondria rather than the cytoplasm or nucleus, thereby deviating from the conventional anticancer mechanism of doxifluridine (*i.e.* TS inhibition). However, it remains unclear whether the observed activation of intrinsic apoptosis is due to mitochondrial localization of doxifluridine or the presence of fluorescent reporter, eithidium. Overall, this report highlights the importance of cancer-targeting units and a stimuli-responsive fluorogenic prodrug approach towards potential anticancer efficacy.

In 2018, Liu and co-workers synthesized a promising anticancer theranostic prodrug **FDU-DB-NO$_2$**, which consists of hypoxia-responsive 4-nitrobenzyl group, a self-immolative fluorescent moiety (CM) for the real-time tracking of the drug uncaging process and the chemotherapeutic drug 5-fluorodeoxyuridine (FDU) (Fig. 5A).[51] FDU, a derivative of **5-FU**, is widely used for the treatment of colorectal, renal, and gastric cancers.[52] The activation mechanism of **FDU-DB-NO2** was confirmed by a significant enhancement in fluorescence emission at 530 nm (Fig. 5B), as well as by HPLC studies, upon incubation with Nitroreductase (NTR) and sodium dithionite ($Na_2S_2O_4$) under hypoxic conditions (1% O_2), respectively. As illustrated in Fig. 5A, **FDU-DB-NO$_2$** is selectively activated under hypoxic conditions, leading to the simultaneous release of the active drug FDU and the fluorescent reporter CM. As predicted, the fluorescence intensity of the released fluorophore (CM) decreased with increasing O_2 concentration in MGC-803 cells, while the fluorescence intensity completely diminished under normoxic conditions, indicating the critical role of hypoxia-associated enzyme NTR in triggering the prodrug activation (Fig. 5C). *In vitro* cytotoxicity studies revealed that **FDU-DB-NO$_2$** exhibited pronounced anticancer activity against gastric carcinoma (MGC-803) and breast cancer (MCF-7) cells under hypoxic conditions (3% O_2), compared to normoxic conditions (20% O_2). Notably, the prodrug showed minimal cytotoxicity towards the normal cell line (BRL-3A, a rat liver-derived cells), further supporting its hypoxia-selectivity. Moreover, treatment of MCF-7 tumour–bearing mice with **FDU-DB-NO$_2$** resulted in a significant reduction in tumour size compared with the control group (Fig. 5D), highlighting the *in vivo* anticancer potential of the prodrug.[51] These results collectively underscore the potential of hypoxia-responsive fluorogenic prodrugs to selectively target hypoxic tumour tissues while minimizing off-target toxicities on normal tissues.

Although ROS act as secondary messengers in signal transduction pathways in healthy normal cells, their levels are

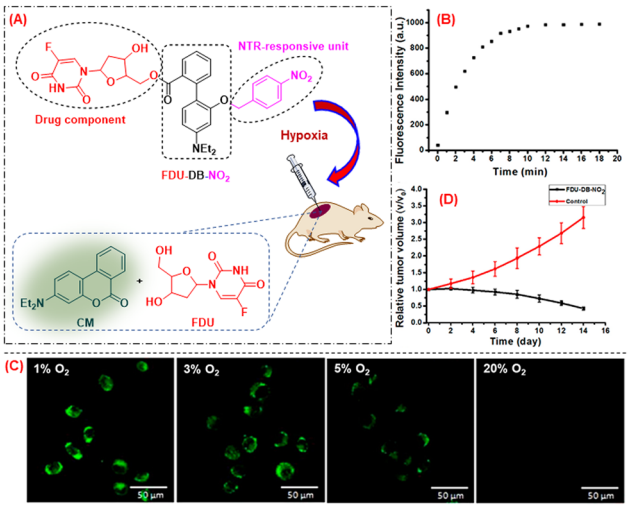

Fig. 5 (A) Proposed mechanism for the hypoxia-induced activation of **FDU-DB-NO$_2$** for the release of CM and FDU. (B) Time-dependent emission intensity at 530 nm upon the incubation of **FDU-DB-NO$_2$** ($\lambda_{ex/em}$ = 380/530 nm) with NTR under hypoxic conditions (1% O_2). (C) Two-photon confocal microscopy images (green channel) of MGC-803 cells incubated with **FDU-DB-NO$_2$** for 12 h under different hypoxic conditions (1% O_2, 3% O_2, and 5% O_2) and normoxic conditions (20% O_2). (D) Relative tumour volume of MCF-7-cell-inoculated xenograft mice treated with **FDU-DB-NO$_2$**. Reproduced with permission.[51] Copyright (B), (C) and (D) 2018, American Chemical Society.

significantly upregulated in the tumour microenvironment due to enhanced metabolic activity and mitochondrial dysfunction.[53] In 2021, Li and co-workers reported a newly synthesized dual-stimuli-responsive theranostic probe **CX-B-DF**, which integrates a near-infrared (NIR)-fluorogenic moiety (**CX-OH**), a H_2O_2-responsive unit (boronate ester), and an inactive drug 5′-deoxy-5-fluorouridine (5′-DFUR or doxifluridine) (Fig. 6A).[54]

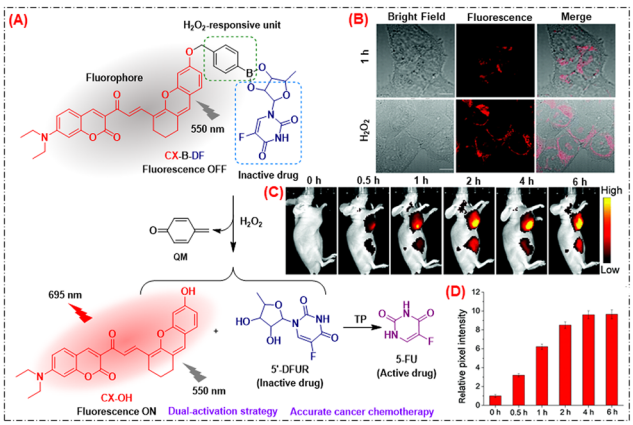

Fig. 6 (A) Schematic representation of ROS-mediated activation of **CX-B-DF**. (B) Fluorescence imaging of **CX-B-DF** (10 μM) in HCT-116 cells. The cells were incubated with **CX-B-DF** for 1 h and the cells were pre-treated with H_2O_2 (50 μM) for 0.5 h and then incubated with **CX-B-DF** for 0.5 h. (C) Fluorescence imaging of tumour-bearing mice after intravenous injection of **CX-B-DF** (200 μM) with time (0 h, 0.5 h, 1 h, 2 h, 4 h and 6 h). (D) Relative pixel intensity in panel (C). Reproduced with permission.[54] Copyright (B), (C) and (D) 2021, The Royal Society of Chemistry.

The authors employed a dual-activation strategy to achieve precise delivery of the chemotherapeutic agent specifically to the cancer cells. In this study, upon exposure to the elevated level of intracellular H_2O_2, the boronate ester moiety of **CX-B-DF** undergoes oxidative cleavage, leading to the release of the active fluorophore (**CX-OH**) along with 5′-DFUR. Subsequently, 5′-DFUR was enzymatically converted by thymidine phosphorylase (TP) to the active anticancer drug **5-FU** within the cancer cells (Fig. 6A). This activation mechanism of the prodrug and the release profile was validated in both *in vitro* and *in vivo* models. Interestingly, the higher level of endogenous ROS in cancer cells over the normal cells was validated by the bio-imaging ability of **CX-B-DF**. While the prodrug exhibited very weak fluorescence emission in normal cells, a significantly increased emission was observed in HCT-116 cancer cells, which was further enhanced upon the addition of exogenous H_2O_2 (Fig. 6B). Moreover, the prodrug exhibited negligible cytotoxicity towards normal cells compared to the cancer cells. This result further correlates with the hypothesis that upon dual activation by H_2O_2 and TP in cancer cells, the prodrug undergoes sequential cleavage to release the active drug **5-FU**, leading to pronounced cytotoxic effects, selectively to cancer cells. Furthermore, **CX-B-DF** enabled real-time fluorescence imaging in tumour-bearing mice, demonstrating high tumour-specific activation and effective suppression of tumour growth *in vivo* (Fig. 6C and D).[54] Overall, this work underscores the importance of the advanced dual-locked fluorogenic prodrug system in enabling precise therapeutic strategies that selectively target tumour tissue while minimizing toxic effects on normal healthy tissue.

Emerging evidence indicates overexpression of alkaline phosphatase (ALP) in several organ-specific cancers, including prostate, pancreatic, breast, lung, ovarian, and gastric cancers, suggesting its potential as a cancer biomarker.[55] In recent years, researchers have also exploited this enzyme as a cancer cell-targeting unit to achieve precise delivery of anticancer drugs to tumour tissues. For instance, in 2023, Venkatesh and co-workers reported the development of a highly water-soluble ALP-responsive fluorogenic prodrug of **5-FU**, called **5-FUPD**.[56] In this work, the authors synthesized the prodrug by conjugating a self-immolative fluorescent reporter (*p*-naphthoquinone methide) to a modified **5-FU** moiety through an ALP-responsive phosphate group (Fig. 7A). The prodrug activation was initiated by ALP-mediated hydrolysis of the phosphate group, followed by a 1,8-elimination of the self-immolative fluorophore, leading to the release of the active drug (**5-FU**) (Fig. 7A). Notably, **5-FUPD** displayed time-dependent activation in the presence of ALP under physiological conditions, as evidenced by a gradual increase in fluorescence intensity at 431 nm (Fig. 7B and C). The authors further investigated the anti-proliferative activity of **5-FUPD** in ALP overexpressing cancer cells, including cervical (HeLa) and liver (HepG2) cancer cells. While the prodrug exhibited significant cytotoxicity against these cancer cells, it was nontoxic to normal liver cells (WRL-68). Interestingly, the authors also reported that the *p*-naphthoquinone methide, released concomitantly with **5-FU** upon ALP-triggered hydrolysis, scavenged intracellular GSH as evidenced by a significant increase in intracellular ROS levels. Furthermore, the biocompatibility of

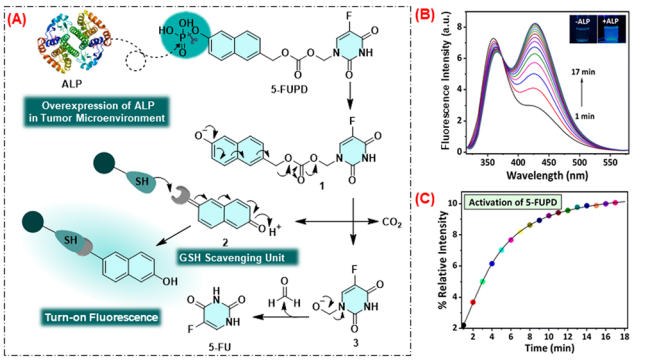

Fig. 7 (A) Proposed mechanism of ALP-catalyzed **5-FUPD** activation. (B) and (C) Emission spectra representing the kinetics of **5-FUPD** activation at pH 7.4 upon incubation with ALP (50 U/L), λ_{em} = 431 nm. Reproduced with permission.[56] Copyright (B) and (C) 2023, The Royal Society of Chemistry.

5-FUPD and the ALP-responsive release of *p*-naphthoquinone methide with turn-on blue fluorescence upon its reaction with cellular abundant biothiols, indicated the theranostic potential of this prodrug.[56] Notably, the coumarin-backbone in the prodrug model served dual roles. It acted as a self-immolative linker, which was finally converted to the turn-on fluorogenic unit. Moreover, the work demonstrates the synergistic role of the released fluorescent reporter in enhancing the chemotherapeutic efficacy of the parent drug, accompanied by turn-on fluorescence while reducing toxicity towards healthy normal cells.

Subsequently, in 2024 our group reported the esterase-responsive self-immolative fluorogenic prodrugs of **5-FU**, namely **BJ-50** and **BJ-92**.[57] The prodrugs were rationally designed wherein an esterase-responsive pivaloyloxymethyl group was linked to a similar coumarin-based self-immolative fluorophore unit, which was coupled to **5-FU**. In prodrug **BJ-50**, **5-FU** was directly attached to the coumarin moiety through a C–N bond, whereas in **BJ-92** a benzylic self-immolative spacer containing a carbonate linker was incorporated between the fluorophore and drug (Fig. 8A). Activation of the prodrugs was attempted using PLE under physiological conditions. Interestingly, while **BJ-92** exhibited a gradual increase in fluorescence intensity at 458 nm, reaching a saturation plateau after 5 h of incubation with PLE, **BJ-50** showed a fixed emission intensity pattern over time (Fig. 8B and C). Based on the fluorescence emission, HPLC and ESI-MS analyses, the mechanistic outlines for the feasibility of turn-on fluorogenic release of **5-FU** from the prodrugs in the presence of PLE was established (Fig. 8D). Upon incubating **BJ-92** with PLE, efficient release of both **5-FU** and the coumarin fluorophore was observed, as illustrated in Fig. 8D. In contrast, under identical conditions, **BJ-50** failed to release the active drug; instead, its reaction with PLE led to the formation of new fluorogenic intermediate **4** that could not undergo self-immolative cleavage due to the presence of the direct C–N bond between **5-FU** and the coumarin ring (Fig. 8D). These observations highlight the importance of selecting suitable functional groups for the coupling of drugs with the self-immolative core for a feasible drug uncaging process upon the activation of the prodrug.

Notably, **BJ-92** exhibited significantly enhanced cytotoxicity in A549 cells compared to the parent drug **5-FU**, while

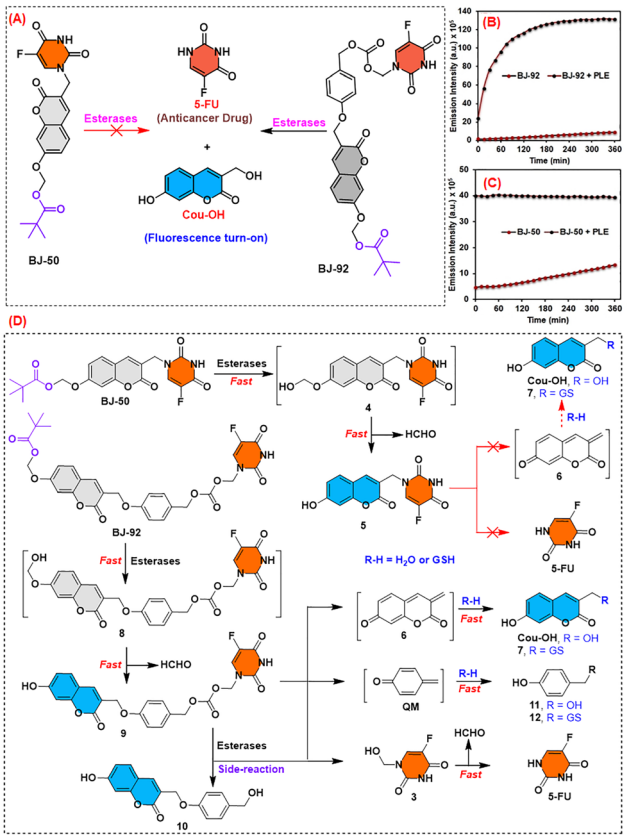

Fig. 8 (A) Schematic representation for the esterase-responsive activation of the prodrugs **BJ-50** and **BJ-92** followed by the feasibility of release of **5-FU** with turn-on fluorescence of **Cou-OH**. Emission spectra of (B) **BJ-92** (10 μM) and (C) **BJ-50** (10 μM) in the presence and absence of PLE (0.5 U mL^{-1}) with variable time (0–360 min). The emission intensity was measured at λ_{em} = 458 nm. (D) Plausible mechanistic pathways for the esterase-mediated activation of **BJ-50** and **BJ-92** and the feasibility of releasing active drug **5-FU** and the fluorophore **Cou-OH**.

minimizing the toxicity in normal human embryonic kidney (HEK-293) cells, indicating improved therapeutic potential (Fig. 9A–C). Additionally, intracellular activation of the prodrug by endogenous esterases was validated through turn-on fluorescence imaging in A549 cells in the presence and absence of a known esterase inhibitor (BNPP) (Fig. 9D). Further mechanistic insights revealed that **BJ-92** exerts its anticancer effect through oxidative stress-mediated DNA damage (downregulation of PARP) and p53-dependent apoptosis, similar to the parent drug, **5-FU**.[57] Collectively, the development of stimuli-responsive fluorogenic prodrugs of TS inhibitors offered a promising platform for precise and personalized cancer therapy with improved bioavailability, enhanced selectivity and reduced side effects, compared to the parent inhibitors.

4. Prodrugs of topoisomerase-II (Topo-II) inhibitors

It has been reported that rapidly proliferating cells undergo frequent cycles of DNA replication, which increases the likelihood of replication errors and consequently places stress on the DNA replication machinery. Replication stress, caused by several endogenous or exogenous factors, thus impairs DNA replication and its repairing processes, leading to the accumulation of mutations that are a fundamental driver of tumourigenesis.[58] This persistent replication stress, an enabling hallmark of cancer cells,[1] has been exploited by researchers for decades as a therapeutic vulnerability in cancer treatment. Therefore, tipping the cancer cells towards a more stressed replicative state through external agents can lead to the collapse of the DNA replication machinery, ultimately resulting in cancer cell death. One of the commonly targeted enzymes of DNA replication is Topo-II. It plays a crucial role in DNA replication by regulating DNA topology, including under-winding, over-winding, knotting and tangling of DNA strands.[59] Mechanistically, topoisomerases reduce torsional strain created by DNA helicases by relaxing the supercoiled DNA. This process involves the formation of a reversible Topo-DNA cleavage complex, resulting in transient DNA double-strand breaks (DSBs). These transient breaks allow the passage of another DNA segment to rejoin the DNA structure, thereby maintaining replication fork progression and genomic integrity.[60] This indispensable function of Topo-II makes it a prominent molecular target for anticancer therapeutics.[61] Moreover, its overexpression in various cancer types, including breast cancer and oral squamous cell carcinoma, provides a potent avenue for targeting the replication machinery in cancer cells.[62,63]

Over the decades, several Topo-II inhibitors have been developed to disrupt the DNA replication machinery in cells. Although Topo-II can be inhibited at multiple points in its enzymatic cycle, its inhibitors are broadly classified into two main categories: catalytic inhibitors and Topo-II poisons (Fig. 10). Importantly, catalytic inhibitors such as dexrazoxane and merbarone exhibit anticancer activity by preventing Topo-II-DNA complex formation, thereby reducing the catalytic activity of Topo-II and producing relatively weak cytotoxicity in cancer cells. In contrast, Topo-II poisons such as doxorubicin, etoposide, daunorubicin and amonafide induce Topo-II-DNA complex formation, leading to the accumulation of DNA DSBs and blocking the replication and transcription (Fig. 10).[19]

Therefore, Topo-II poisons cause DNA-damage mediated cell death, resulting in pronounced cytotoxicity and anticancer effects. Although many Topo-II poisons are FDA-approved anticancer agents, their clinical applications are often limited due to undesired side effects and poor bioavailability. For instance, the clinical utility of doxorubicin is limited due to drug-induced cardiotoxicity, whereas etoposide is constrained by its poor aqueous solubility.[64,65] Therefore, substantial research attention has been devoted towards the development of prodrugs of different Topo-II inhibitors for anticancer therapy.

Over the past decade, several small-molecule prodrugs of doxorubicin have been designed incorporating different stimuli-responsive linkers, including enzyme-, ROS- and pH-responsive moieties, primarily focusing on target-specific doxorubicin delivery in the tumour microenvironment (Fig. 11). For instance, in 2018, Kim and co-workers reported a β-galactosidase-activated

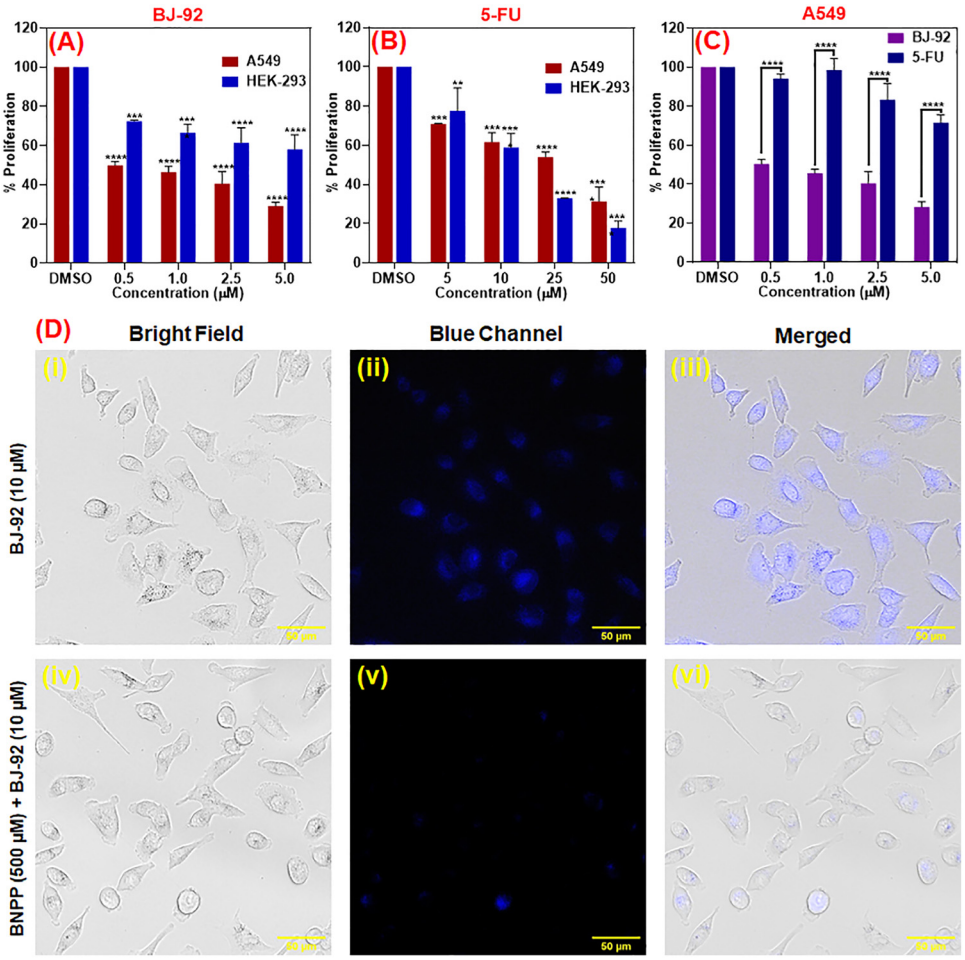

Fig. 9 (A) and (B) Dose-dependent anti-proliferative activity of **BJ-92** and **5-FU** in A549 and HEK-293 cells. (C) Comparative anti-proliferative activity of **BJ-92** and **5-FU** in A549 cells. (D) Fluorescence microscopy images (bright field, blue channel, and merged) of A549 cells in the presence of (i)–(iii) **BJ-92** (10 μM) after incubation for 3 h and (iv)–(vi) after pre-incubation with BNPP (500 μM) for 4 h followed by incubation with **BJ-92** (10 μM) for 3 h. Scale bar: 50 μm.

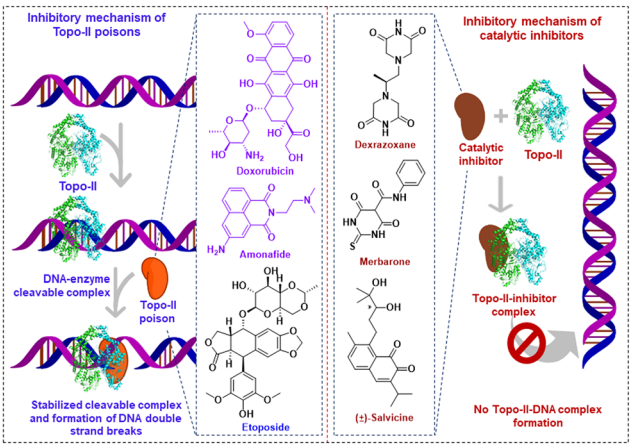

Fig. 10 Chemical structures of representative Topo-II poisons and Topo-II catalytic inhibitors highlighting their inhibitory mechanisms.

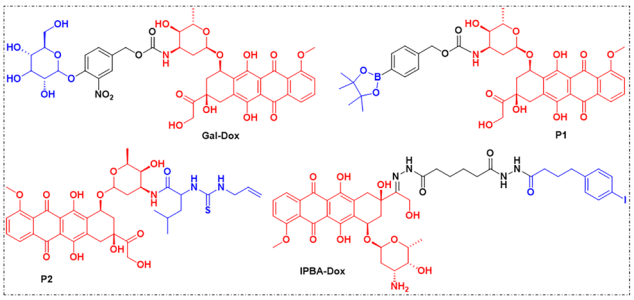

Fig. 11 Chemical structures of representative stimuli-responsive prodrugs of doxorubicin.

prodrug of doxorubicin (**Gal-Dox**) for the selective delivery of doxorubicin in asialoglycoprotein overexpressing colon cancer cells.[66] In the following year (2019), Labruère and his group developed H_2O_2-responsive doxorubicin prodrugs (**P1**) and systematically investigated the role of self-immolative linkers in organ-specific cancer cells, facilitating the efficient release of doxorubicin with effects comparable to those of the free drug.[67] In the same year, Krasnovskaya and co-workers synthesized a

pH-responsive dual prodrug (**P2**) system comprising doxorubicin and albutoin, demonstrating around 30-fold reduction in cytotoxicity under physiological conditions (pH 7.6) compared to mildly acidic tumor-like conditions (pH = 6.6) in PC-3 cells.[68] Furthermore, in 2023, Williams and co-workers designed a pH-responsive albumin-binding doxorubicin prodrug (**IBPA-Dox**) to amplify cellular uptake and improve pharmacokinetic profiles by the enhancement of binding affinity towards human serum albumin (HSA).[69] Despite these advances, these reports fail to address strategies for mitigating doxorubicin-related side effects in cardiac cells; consequently, the clinical translation of doxorubicin remains constrained by its cardiotoxicity. Therefore, a deeper mechanistic understanding and rational design of prodrug systems aimed at alleviating doxorubicin-induced cardiotoxicity represents a critical direction for future research.

Amonafide, a naphthalimide-based Topo-II poison, failed to advance beyond phase III clinical trials due to altered metabolism, despite exhibiting potent anticancer activity. Notably, amonafide is metabolized to the toxic *N*-acetyl amonafide by *N*-acetyltransferase 2 (NAT2), resulting in slower plasma clearance and accumulation of both compounds, leading to adverse hematological side effects in patients.[19] To overcome this limitation, significant efforts have been dedicated to developing stimuli-responsive prodrugs of amonafide by functionalizing the free primary amino group, resulting in improved bioavailability and reduced systemic toxicity.

In 2021, Qian and co-workers reported a H_2S-responsive fluorogenic prodrug of amonafide **PNF** (Fig. 12A).[70] H_2S is a gasotransmitter involved in the regulation of several biological processes; however, its levels are elevated in cancer cells, where it promotes cancer development in a concentration-dependent manner.[71] The H_2S-activated release of amonafide from **PNF** was confirmed by fluorescence spectroscopy with a strong fluorescence emission at 598 nm in response to NaHS (Fig. 12B). The prodrug was screened for its anticancer activity in different organ-specific cancer cells, including cisplatin-resistant cells (A549R, A2780R). Notably, **PNF** exhibited potent cytotoxicity across all the tested cancer cell lines, with IC_{50} values in the low micromolar range. Moreover, **PNF** showed 6-fold greater potency against the cisplatin-resistant cell line A549R than the parent drug amonafide.

Notably, **PNF** exhibited significantly enhanced fluorescence intensity in the cisplatin-resistant A549R cells upon the treatment of exogenous NaHS and sodium nitroprusside (stimulus for endogenous H_2S production). Importantly, the authors reported that **PNF** released amonafide in the presence of lysosomal H_2S after 6 h of incubation and translocated to the nucleus after a prolonged incubation for 24 h. Based on these observations, the authors concluded that **PNF** exhibits anticancer activity by inducing autophagy within lysosome, followed by its translocation to the nucleus leading to DNA damage-mediated arrest of cells in the G2/M phase of the cell cycle, ultimately resulting in the death of cisplatin-resistant cancer cells (Fig. 12C).[70] However, endogenous H_2S levels are highly dynamic in nature and tightly regulated by the redox status of the cellular environment.[73] Therefore, H_2S-responsive prodrugs may exhibit limited selectivity toward cancer cells.

In 2022, Scanlan and co-workers reported two glycosidase-responsive prodrugs of amonafide (**13-14**) towards their anticancer activities to facilitate selective activation in the enzyme-overexpressed tumour microenvironment.[72] Notably, glycosidases are known to be overexpressed in various inflammatory conditions, including various cancers, thereby making them attractive targets for the development of enzyme-activated theranostic agents.[24] The enzymatic activation of prodrugs and the release of amonafide was confirmed using spectroscopic studies, wherein the activation process was proposed to involve the hydrolysis of glycosidic bonds in the presence of glycosidases (β-galactosidase or β-glucuronidase) (Fig. 12D). The turn-on fluorescence in the cellular medium (HeLa cells) in the presence and absence of exogenous enzymes revealed green fluorescence in the cytosol in the presence of exogenous enzymes (Fig. 12E).

The evaluation of the anti-proliferative activity of the prodrugs in HeLa, HCT-116 and HepG2 cells revealed potent cytotoxicity of the β-galactosidase-sensitive prodrug **13**. In contrast, the β-glucuronidase-sensitive prodrug **14** was nontoxic under identical conditions. These results suggest that the prodrug **13** undergoes intracellular metabolism by β-galactosidase to release amonafide with potent anticancer activity. However, the cytotoxicity of both the prodrugs was increased significantly in the presence of exogenous enzymes. Collectively, this report focuses on the delivery of amonafide *via* activation of endogenous/exogenous glycosylated enzymes, especially in bio-imaging studies. Nevertheless, for more efficacious delivery of amonafide, further exploration of advanced prodrug strategies that emphasize

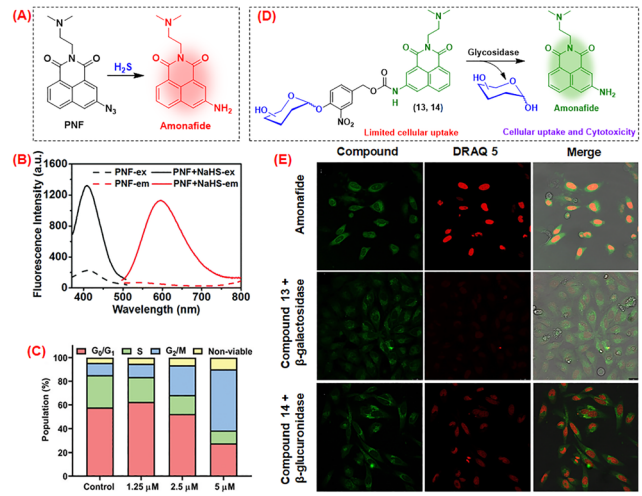

Fig. 12 (A) Schematic representation of the H_2S-responsive activation of the prodrug **PNF**. (B) Excitation and emission spectra of **PNF** in the presence and absence of NaHS (H_2S donor). (C) Cell cycle arrest of A549R cells in the presence of **PNF** after 24 h of incubation. (D) Glycosidase-mediated release of amonafide from prodrugs **13** and **14**. (E) Fluorescence microscopy images of HeLa cells in the presence of Amonafide (50 μM), prodrug **13** (50 μM) with β-galactosidase (1 U), and prodrug **14** (50 μM) with β-glucuronidase (1 U). Reproduced with permission.[70] Copyright (B) and (C) 2021, The Royal Society of Chemistry. Reproduced with permission.[72] Copyright (E) 2022, Wiley-VCH GmbH.

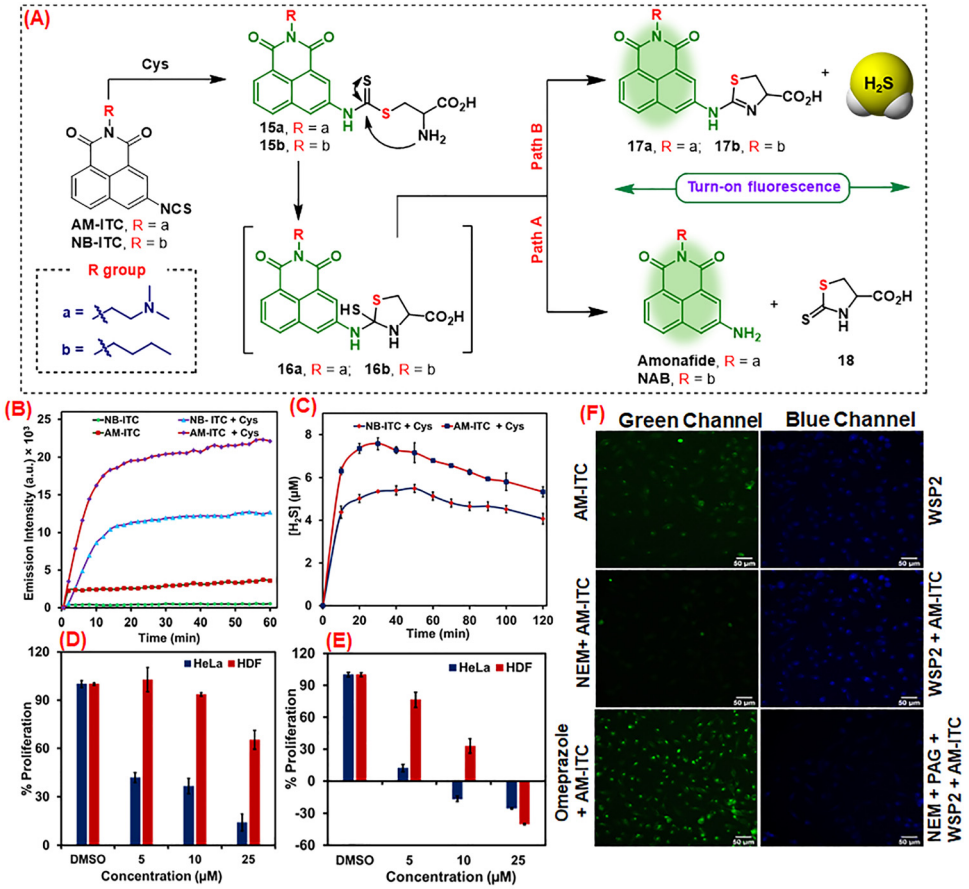

Fig. 13 (A) Proposed mechanistic pathways for the release of amonafide/NAB and H_2S in the presence of Cys from the prodrugs **AM-ITC** and **NB-ITC**, respectively. (B) Emission spectra of **AM-ITC** and **NB-ITC** (5 μM) in the presence and absence of Cys (200 μM) over 60 min. (C) The H_2S release profile of **AM-ITC** and **NB-ITC** (25 μM) in the presence of Cys (1 mM) over 120 min using an MB assay. Relative anti-proliferative activity of (D) **AM-ITC** and (E) amonafide in HeLa and HDF cell lines. (F) Fluorescence microscopy images (green and blue channels) of HeLa cells in the presence of **AM-ITC** (25 μM) for confirming the adjuvant cellular release of amonafide (green) and H_2S (blue). The release of H_2S was confirmed by using the H_2S-sensitive probe **WSP2**. Scale bar: 50 μm.

on activation by endogenous bio-analytes, along with detailed biological evaluation, would be necessary.

In 2023, our group developed a cysteine (Cys)-responsive isothiocyanate-based prodrug **AM-ITC** capable of co-delivering amonafide and H_2S with the aim of understanding the impact of H_2S on amonafide-induced cytotoxicity (Fig. 13A).[74] A control prodrug **NB-ITC** was also synthesized to understand the effect of the released H_2S as the prodrug **NB-ITC** would not release amonafide, but rather a structural analogue (Fig. 13A). H_2S is known to exert a cytoprotective effect in healthy cells against the adverse side effects of anticancer agents by regulating the intracellular antioxidant defence system.[75] Therefore, researchers have focused significantly on adjuvant delivery of H_2S with existing chemotherapeutic drugs. The sensitivity and selectivity of **AM-ITC** and **NB-ITC** towards different biothiols revealed that the prodrugs could be activated only by Cys. Interestingly, the highly electrophilic isothiocyanate group rapidly reacted with Cys with the release of amonafide and its analogue from **AM-ITC** and **NB-ITC**, respectively within 10–15 min (Fig. 13B). Moreover, the release of H_2S from **AM-ITC** and **NB-ITC** was confirmed using a Methylene Blue (MB) assay over a period of 120 min, confirming the potential of the prodrugs **AM-ITC** and **NB-ITC** to co-deliver amonafide/NAB and H_2S upon Cys-mediated activation (Fig. 13C). The nucleophilic attack of Cys at the electrophilic isothiocyanate group led to the formation of the corresponding Cys-adducts as transient intermediates, which undergo intramolecular cyclization to generate cyclic intermediates **16a/16b**. These intermediates subsequently decompose to release free drugs and H_2S along with the by-products.

The importance of prodrug design and the cytoprotective effect of the released H_2S were investigated next by evaluating their anti-proliferative activities in cancer cells (MDA-MB-231 and HeLa) and non-malignant cells (HDF). Although **AM-ITC** exhibited relatively lower anti-proliferative activity in cancer cells compared to free amonafide, a more pronounced cytoprotective effect was observed in the non-malignant cells (Fig. 13D and E). These observations highlight the cytoprotective effect of H_2S in mitigating amonafide-induced toxicity towards normal cells. Next, the release of amonafide as well as H_2S in the cellular medium was evidenced using fluorescence microscopy

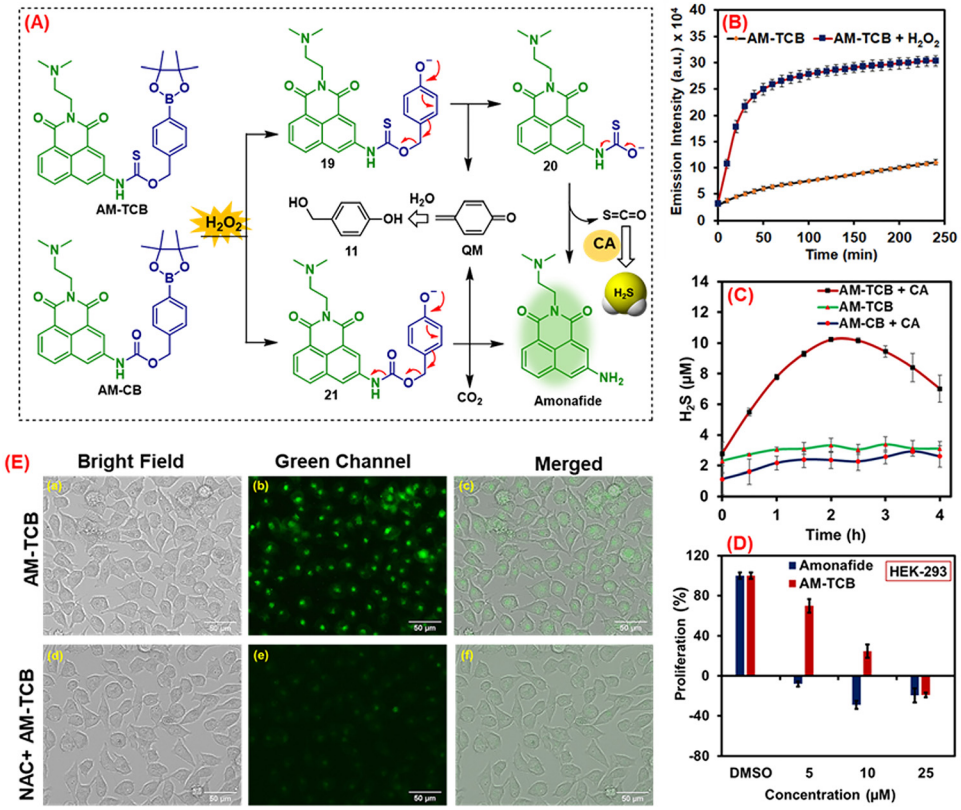

Fig. 14 (A) Proposed mechanism for the release of amonafide and H_2S from **AM-TCB** and amonafide from **AM-CB** in the presence of H_2O_2 and CA. (B) Emission spectrum of **AM-TCB** (5 μM) in the absence and presence of H_2O_2 (200 μM) over 240 min for the release of self-reporting drug amonafide (λ_{em} = 575 nm). (C) Feasibility of time-dependent H_2S release from **AM-TCB** (50 μM) and **AM-CB** (50 μM) in the presence of H_2O_2 (100 μM) and CA (50 μg mL^{-1}) over 4 h. (D) The relative anti-proliferative activity of amonafide and **AM-TCB** in HEK-293 cells. (E) Fluorescence microscopy images of HeLa cells (a)–(c) incubated with **AM-TCB** (25 μM) and (d)–(f) pre-incubated with NAC (2 mM) followed by the treatment of **AM-TCB** (25 μM).

(Fig. 13F). The Cys-mediated release of amonafide in HeLa cells was further confirmed by pre-treating cells with the thiol-enhancer omeprazole and thiol-quencher *N*-ethylmaleimide (NEM). Notably, a significant green fluorescence was indicative of the release of free amonafide. Moreover, the release of H_2S from **AM-ITC** in HeLa cells was confirmed by the intense blue fluorescence in the presence of the H_2S-responsive probe **WSP2** (Fig. 13F). Taken together, this work reveals a novel approach for the adjuvant delivery of amonafide with H_2S to mitigate the amonafide-mediated side effects in normal cells.[74]

The development of **AM-ITC** provided us with important information about the feasibility of adjuvant delivery of amonafide and H_2S to mitigate the side effects of amonafide. However, due to the presence of the isothiocyanate group in **AM-ITC**, the prodrug becomes highly reactive, facilitating rapid nucleophilic reactivity and losing selectivity. Moreover, due to the low intracellular abundance of Cys, the activation strategy of the amonafide prodrug with an isothiocyanate-based reactive group was further improved with a more advanced prodrug strategy. Therefore, in our next strategy, we developed a dual bioanalyte (H_2O_2 and carbonic anhydrase, CA)-triggered thiocarbamate-based hybrid prodrug (**AM-TCB**) for the sustained release of amonafide and H_2S, accompanied by turn-on fluorescence (Fig. 14A).[76] A carbamate-based control prodrug, **AM-CB**, was also designed, which could release only amonafide without releasing H_2S, thus supporting the CA-mediated H_2S release from the thiocarbamate-based prodrug **AM-TCB** (Fig. 14A). While the release of amonafide from **AM-TCB** was confirmed in the presence of H_2O_2 using analytical methods, the release of H_2S from the prodrug was confirmed using the MB assay in the presence of both the analytes, such as H_2O_2 and CA (Fig. 14B and C). While the activation of **AM-TCB** by H_2O_2 generates carbonyl sulfide (COS) and amonafide, a subsequent decomposition of COS by CA generates H_2S. In contrast, the carbamate-based prodrug **AM-CB** generates amonafide without any H_2S (Fig. 14C).

The prodrug **AM-TCB** was further studied for its anti-proliferative activity in both cancer cell lines (HeLa and MDA-MB-231) and normal cells (HEK-293). **AM-TCB** exhibited lower cytotoxicity in cancer cell lines than free amonafide. Similarly, its toxicity in HEK-293 cells was also reduced relative to free amonafide, indicating the cytoprotective role of H_2S in alleviating the toxicity of the released amonafide (Fig. 14D). Additionally, the intracellular release of the self-reporting fluorogenic drug amonafide and the gasotransmitter H_2S was confirmed by fluorescence microscopy images. An intense green fluorescence in HeLa cells upon treatment with **AM-TCB**

indicates intracellular H_2O_2-triggered activation (Fig. 14E). Furthermore, intracellular H_2S release was confirmed by the intense blue fluorescence, which was observed upon the co-incubation of HeLa cells with **AM-TCB** and the H_2S-responsive fluorogenic probe **WSP2**. Moreover, the prodrug **AM-TCB** exhibited similar regulation of p53 and Bcl2 as amonafide, suggesting that the released amonafide is responsible for exerting an anticancer effect in MDA-MB-231 cells. Altogether, the mitigation of amonafide-induced toxicity in normal cells has been explored *via* concomitant release of H_2S and amonafide from both **AM-ITC** and **AM-TCB**. These findings underscore a promising avenue for adjuvant drug delivery strategies that integrate both a single stimulus and dual-locked mechanism. However, a more comprehensive mechanistic insight into ROS-responsive drug release remains essential for the strategic design of advanced and more effective prodrug systems for cancer therapy.

In 2024, Yin and co-workers designed ROS-responsive prodrugs of amonafide, namely **PBE-AMF** and **PBA-AMF**, consisting a boronic ester and boronic acid group, respectively Fig. 15A.[77] While both the prodrugs reacted with H_2O_2 with the release of amonafide, the boronic ester (PBE)-containing prodrug **PBE-AMF** undergoes hydrolysis under physiological conditions to form the corresponding boronic acid derivative (PBA) and exhibits poor aqueous solubility. Activation of **PBA-AMF** by ROS leads to the self-immolative process and releases the active drug amonafide (Fig. 15B). Upon confirming the release of amonafide, the authors investigated the comparative anti-proliferative activities of **PBE-AMF** and **PBA-AMF** in MDA-MB-231 cells. The results revealed more efficient sialic acid (SA)-mediated uptake of **PBA-AMF** by MDA-MB-231 cells than **PBE-AMF**, resulting in enhanced cytotoxicity. However, this trend is reversed when the cells are pre-treated with 3A-PBA, a competitive inhibitor of SA. These findings confirmed that the superior activity of **PBA-AMF** over **PBE-AMF** arises from the SA binding ability of the PBA moiety over the PBE group, as well as the poor aqueous solubility of **PBE-AMF** at physiological pH. Therefore, **PBA-AMF** was chosen for further investigations. The release of amonafide in the cellular medium was visualized by the intense red fluorescence of amonafide in MDA-MB-231 cells, and ROS-mediated release was confirmed by fluorescence quenching upon the pre-treatment of cells with NAC and an enhanced fluorescence on pre-treatment with lipopolysaccharide (LPS) or H_2O_2 (Fig. 15C).

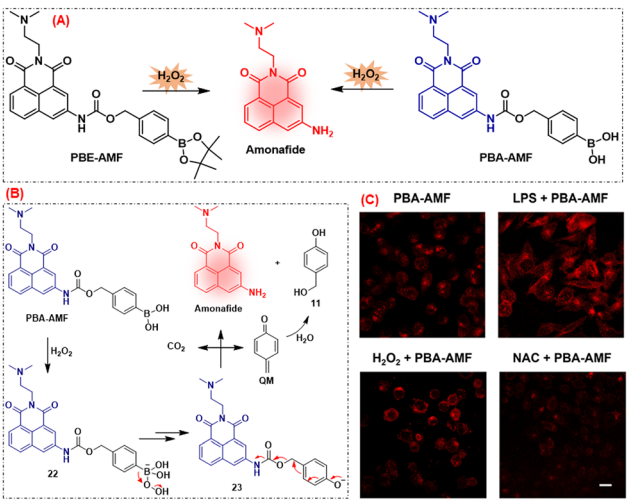

Fig. 15 (A) Schematic representation of the H_2O_2-mediated activation of **PBE-AMF** and **PBA-AMF** with the release of amonafide. (B) The release mechanism of amonafide from **PBA-AMF** in the presence of H_2O_2. (C) Confocal images of MDA-MB-231 cells after incubating with **PBA-AMF**, LPS + **PBA-AMF**, H_2O_2 + **PBA-AMF**, and NAC + **PBA-AMF** for 6 h. Scale bar: 20 μm. Reproduced with permission.[77] Copyright (C) 2024, Elsevier.

In the same year (2024), Qian and co-workers reported a newly synthesized enzyme-responsive prodrug of amonafide, **AcKLP**, with an advanced strategy of a dual-lock technique for the treatment of glioblastoma (Fig. 16A).[78] Notably, histone deacetylase (HDAC) and cathepsin L (CTSL) are overexpressed in glioblastoma, which are able to deacetylate and cleave at a specific site of the peptide chain. The mechanistic investigation revealed that upon HDAC-catalyzed deacetylation of the short peptide, lysine is generated, which is subsequently cleaved by CTSL, leading to the release of free amonafide. Additionally, the authors reported a cysteine-responsive control prodrug of amonafide, **PhTLP**, for comparative understanding (Fig. 16A). Interestingly, the dual enzyme-responsive prodrug **AcKLP** exhibited very high selectivity (SI $>$ 44) towards glioblastoma cells (U87) overexpressing HDAC and CTSL compared to normal HUVEC cells. However, **PhTLP** exhibited comparable toxicity in both U87 and HUVEC cells, with a very low SI of 0.47, indicating the superior selectivity of the enzyme-responsive prodrug toward cancer cells. Furthermore, the intracellular release of the self-reporting fluorogenic amonafide from **AcKLP** was evaluated in U87 cells using fluorescence imaging. A time-dependent increase in red fluorescence was observed, with co-localization within lysosome (Fig. 16B). Importantly, HDAC- and CTSL-mediated release of amonafide from **AcKLP** was confirmed by significant quenching of the red fluorescence in the presence of the HDAC inhibitor SAHA and CTSL inhibitor E64D. These observations further validated that the combined action of HDAC and CTSL is essential for the release of free amonafide from **AcKLP**. Mechanistic studies revealed that **AcKLP** induced

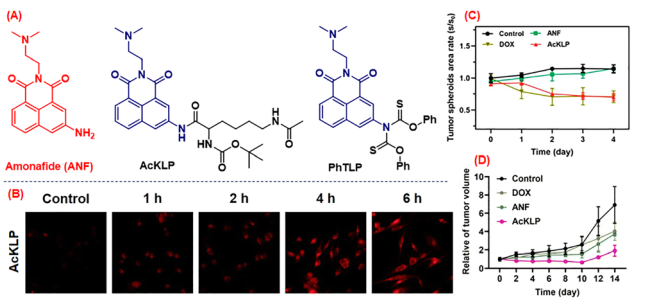

Fig. 16 (A) Chemical structures of amonafide and the prodrugs **AcKLP** and **PhTLP**. (B) Confocal microscopy images of U87 cells treated with **AcKLP** (5 μM) at different time points. Scale bar: 20 μm. (C) The volume changes of 3D tumour spheroids under different conditions with an extended incubation time from 0 to 4 days. (D) Relative tumour volumes of different treated groups over 14 days of treatment. Reproduced with permission.[78] Copyright (B), (C) and (D) 2024, The Royal Society of Chemistry.

autophagy-mediated cell death in U87 cells, as evidenced by the upregulation of autophagy marker LC3-I and LC3-II. The anticancer activity of **AcKLP** was further corroborated in a 3D spheroid model, where a significant reduction in spheroid size was observed (Fig. 16C). Moreover, *in vivo* studies in a U87 tumour-bearing xenograft model revealed significant tumour growth inhibition with reduced systemic toxicity, indicating good biocompatibility of **AcKLP** under *in vivo* conditions (Fig. 16D).[78] Taken together, this work emphasizes the advantage of dual-locked enzyme-responsive prodrugs over bioanalyte-responsive prodrugs, owing to the overexpression of specific enzymes in cancer cells and the superior substrate specificity, thereby enabling improved cancer treatment efficacy while minimizing dose-limiting cytotoxicity.

Altogether, the advancement of amonafide-based prodrugs up to 2025 has largely been confined to strategies targeting overexpressed enzymes and bioactive small-molecules, predominantly under normoxic tumour conditions. However, the tumour microenvironment is intrinsically heterogeneous, characterized by dynamic gradients between normoxia and hypoxia.[79] Therefore, hypoxic conditions within the tumour microenvironment play a critical role in modulating therapeutic efficacy. This year (2026), Lee and co-workers developed hypoxia- and H_2S-responsive prodrugs of amonafide (**Amo-c-NO$_2$**, **Amo-NO$_2$**, **Amo-c-N$_3$**, **Amo-N$_3$** and **Amo-M**) for their selective activation within the tumour microenvironment (Fig. 17A).[80] The prodrugs were investigated for their activation and the release of amonafide in the presence of NTR and H_2S. Interestingly, **Amo-c-NO$_2$** exhibited a rapid increase in fluorescence signal upon activation by NTR, reaching a saturation plateau within 20 min (Fig. 17B). As illustrated in Fig. 17C, NTR catalyzes the reduction of **Amo-c-NO$_2$** to generate a 4-aminobenzyl intermediate, which subsequently undergoes self-immolative cleavage to release free amonafide. The authors evaluated the cytotoxicity of prodrugs in a panel of cancer and normal cells and notably, **Amo-c-NO$_2$** exhibited the highest selective cytotoxicity in HCT-116 cells compared to normal cells. Furthermore, **Amo-c-NO$_2$** induced DNA-damage-mediated apoptotic cell death in HCT-116 cells under normoxic conditions, as evidenced by the dose-dependent cleavage of PARP. Interestingly, it was initially localized in the cytoplasm and slowly translocated to the nucleus after 8 h, confirming the DNA-damage mediated cell death of HCT-116 cells. Since NTR is overexpressed in hypoxic conditions, NTR-mediated release of amonafide from **Amo-c-NO$_2$** was explored *via* fluorescence imaging under hypoxia and confirmed by the attenuated fluorescence signal observed in the presence of the NTR inhibitor, dicoumarol, under identical conditions. Intriguingly, while free amonafide exhibited minimal activity against HCT-116, **Amo-c-NO$_2$** showed enhanced potency in HCT-116 cells under hypoxic conditions (Fig. 17D). Moreover, significant tumour growth inhibition was observed in a mouse model, along with no noticeable impact on body weight, thereby suggesting **Amo-c-NO$_2$** as one of the promising prodrugs for targeted delivery of amonafide with reduced systemic toxicity (Fig. 17E).[80]

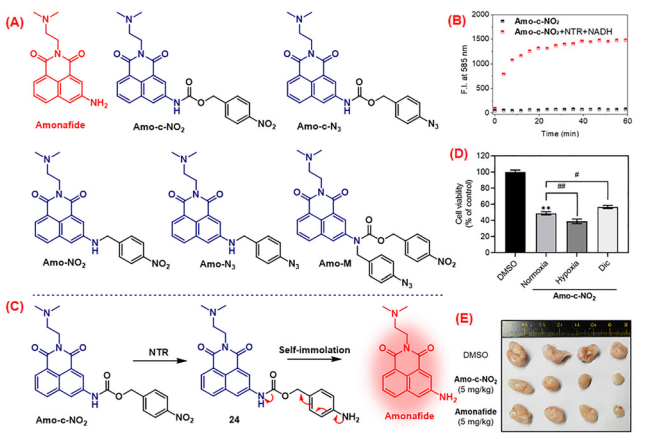

Fig. 17 (A) Chemical structures of amonafide and the synthesized prodrugs **Amo-c-NO$_2$**, **Amo-c-N$_3$**, **Amo-NO$_2$**, **Amo-N$_3$** and **Amo-M**. (B) Time-dependent fluorescence intensity of amonafide at 585 nm in the presence and absence of NTR (5 μg mL^{-1}) and NADH (500 μM). (C) Proposed mechanism of NTR-mediated conversion of **Amo-c-NO$_2$** to amonafide. (D) %Cell viability of HCT-116 cells treated with **Amo-c-NO$_2$** (5 μM) in the presence or absence of dicoumarol (Dic, 5 μM), followed by incubation under hypoxic or normoxic conditions for 24 h. (E) Representative images of tumour tissues of **Amo-c-NO$_2$**-treated mice. Reproduced with permission.[80] Copyright (B), (D) and (E) 2026, Elsevier.

Overall, these reports highlight the sequential advancement of prodrug delivery strategies from small bioactive molecule-triggered systems to dual-enzyme-responsive lockable prodrug systems, focusing on enhancing the bioavailability, tumour selectivity and therapeutic efficacy of amonafide. Furthermore, the prodrug design has been extended to the complex hypoxic environment for the targeted delivery of amonafide under low-oxygen conditions. Such next-generation prodrug systems may enable rational combination therapies, reduce systemic toxicity and assist with spatiotemporal delivery of amonafide for effective cancer treatment.

5. Prodrugs of glutathione-*S*-transferase (GST) inhibitors

Over the decades, GSTs have remained a topic of considerable interest among cancer researchers owing to their controversial roles in cytoprotection and detoxification, as they facilitate the elimination of toxic compounds while contributing to altered drug metabolism and the development of chemoresistance.[81] GSTs are members of the phase II metabolic enzymes that catalyze the conjugation of reduced glutathione (GSH) to a wide range of xenobiotics, thereby promoting their detoxification and facilitating elimination *via* bile excretion or renal transport.[82] This activity emphasizes the paramount cytoprotective function of GSTs, which protect cellular DNA from oxidative damage and mutagenesis. While the widely accepted cytoprotective role of GSTs reflects their function as a cellular ''housekeeper'' in healthy cells, the same activity can paradoxically confer chemoresistance to chemotherapeutic drugs in various organ-specific cancers. Accumulating evidence indicates that GST isozymes are overexpressed in various human cancer cell

lines at both transcriptional and translational levels.[83] These isozymes are divided into seven structurally and functionally distinct classes, namely, α (alpha), μ (mu), π (pi), θ (theta), σ (Sigma), ζ (zeta), and ω (omega).[83] Among these, GSTP1 from the pi-class has been reported to be aberrantly overexpressed across a variety of cancers, including those of the bladder, ovarian, breast, prostate, gastric, and neuroglioma, thereby contributing to resistance to chemotherapeutic agents such as carboplatin, doxorubicin, cisplatin, 5-fluorouracil and others.[84] Mechanistically, the catalytic domain of GSTP1 facilitates the nucleophilic attack of GSH, bound at the G-site of the enzyme subunit, on the electrophilic substrate positioned at the H-site, resulting in the formation of a glutathione-adduct that is subsequently effluxed out of the cells *via* specific transporters (Fig. 18).[85] Thereupon, the overexpression of GSTs contributes to chemotherapeutic drug resistance by working in association with efflux transporters and multidrug resistance proteins. In addition, GSTs are critically involved in several biological processes, particularly redox regulation and intracellular signal transduction.[82] For instance, GSTP1 is known to inhibit c-Jun N-terminal kinase (JNK), a member of the mitogen-activated protein (MAP) kinase signaling pathway. It has been reported that GSTP1 disrupts the interaction between JNK and its downstream substrate c-Jun, by forming a heterotrimeric GSTP1–JNK–c-Jun complex. This interaction acts as a negative regulator of the pro-apoptotic JNK pathway, as the complex impedes JNK activation and inhibits JNK-mediated phosphorylation of c-Jun, thereby attenuating apoptotic signaling (Fig. 18).[86] Furthermore, GSTs are well recognized for their role in modulating pro-apoptotic signaling pathways through post-translational modifications of target proteins, such as *S*-glutathionylation of substrates including p53, peroxiredoxin-VI, ERGIC-STING1 and others.[87] These regulatory functions of GSTP1 highlight its dual role in modulating both cell survival pathways and chemotherapeutic responses in tumour cells. Therefore, GSTP1 represents a promising target for the development of inhibitors that may not only enhance the efficacy of the existing anticancer drugs but also serve as potent therapeutic agents.

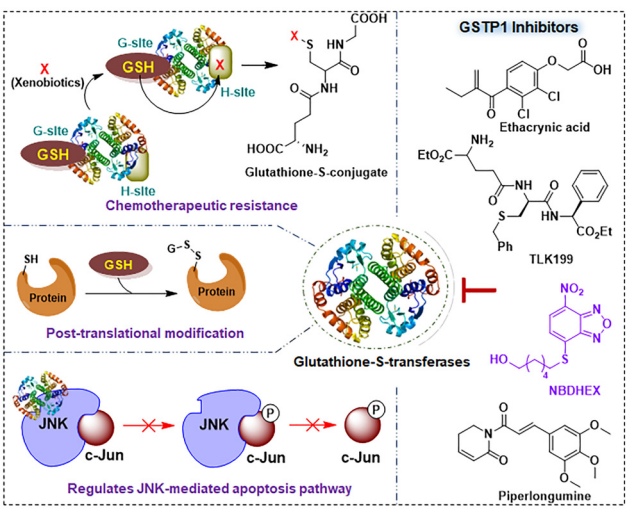

Fig. 18 Schematic representation of GST-mediated chemotherapeutic resistance, post-translational modifications and the regulation of JNK-mediated apoptosis. Chemical structures of some representative inhibitors of GSTP1.

In recent years, various GSTP1 inhibitors have been investigated and developed, and new compounds continue to be synthesized through structural modification of previously reported inhibitors to achieve better specificity towards GSTP1. While ethacrynic acid is FDA-approved with GSTP1 inhibitory activity, ezatiostat (TLK199) and its active metabolite TLK117 have progressed to clinical trials, whereas NBDHEX and piperlongumine remain in the preclinical stage of development (Fig. 18).[88,89] Surprisingly, NBDHEX has gained worldwide recognition as one of the most potent inhibitors of GSTP1, exhibiting pronounced anticancer activity.[90,91] However, its therapeutic application is limited by several drawbacks, including poor selectivity between cancerous and normal cells, low aqueous solubility, and systemic toxicity. Therefore, to overcome these limitations, researchers have pursued various structural modification of NBDHEX mainly with the functionalization at the alkyl side chain. Additionally, initiatives were taken to conjugate it with chemotherapeutic drugs to enhance its anticancer efficacy across a variety of cancer cell lines, and to develop fluorogenic prodrugs of NBDHEX for real-time monitoring and sustained drug release.

In recent years, two Pt(IV) prodrugs of the NBDHEX derivative were reported that involved cisplatin and carboplatin as Pt(II) drugs. The prodrugs were found to have the potency to combat the GST-mediated resistance to Pt(II)-based drugs.[16,17] Although numerous studies have reported NBDHEX derivatives with different structural modifications aimed at improving bioavailability and anticancer efficacy, these derivatives still lack sufficient selectivity towards cancer cells.[92–94] Considering these observations, in recent years, researchers have focused on developing NBDHEX prodrugs with a better selectivity and real-time monitoring of drug activation in the cellular context. In this regard, in 2024 our group rationally designed and reported a newly synthesized biothiol-responsive prodrug of NBDHEX, **RK-296** (Fig. 19A).[95] Activation of **RK-296** by biothiols (GSH) with the release of Biot-NIR-OH and NBDHEX was established in aqueous medium using UV-Vis, and fluorescence methods (Fig. 19B and C). However, a partial release of NBDHEX from the prodrug was observed, as confirmed by HPLC analysis. The work employs GSH as the stimulus as it is the most abundant intracellular thiol, playing an important role in the cellular redox balance, and is present at elevated levels in tumour cells as compared to normal cells.[96] Based on the results from the analytical studies, the biothiol-responsive activation of **RK-296** and the release of the active drug and the fluorophore was proposed (Fig. 19D). Notably, the nucleophilic attack of a biothiol (RSH) may take place at both the S-centres of the unsymmetrical disulfide linkage in **RK-296** as per paths A and B leading to the final release of NBDHEX and the fluorophore.

With this confirmation in hand, the prodrug was evaluated for its time-dependent anticancer activity (48, 72 and 96 h) and

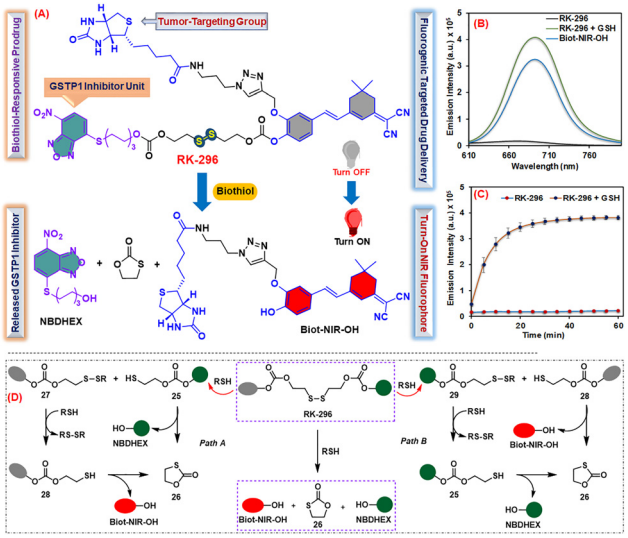

Fig. 19 (A) Biothiol-responsive activation of the prodrug **RK-296** for the release of NBDHEX (GSTP1 inhibitor), with turn-on NIR fluorescence. (B) Emission spectra and (C) Emission kinetics of **RK-296** (10 μM) in the presence/absence of GSH (500 μM). (D) Proposed mechanism for the biothiol-triggered activation of **RK-296** and the release of NBDHEX and Biot-NIR-OH.

compared with free NBDHEX. Notably, it exhibited moderate anti-proliferative activity in MDA-MB-231 cells, consistent with sustained intracellular release of NBDHEX (Fig. 20A and B). The moderate anti-proliferative activity of **RK-296** in cancer cells could be attributed to the partial release of NBDHEX from the prodrug over time. Additionally, the activation of **RK-296** by intracellular biothiols and the turn-on fluorescence was evaluated in HeLa cells using fluorescence microscopy. The prodrug exhibited intense red emission, indicating successful activation of **RK-296** by the endogenous biothiols (Fig. 20C).

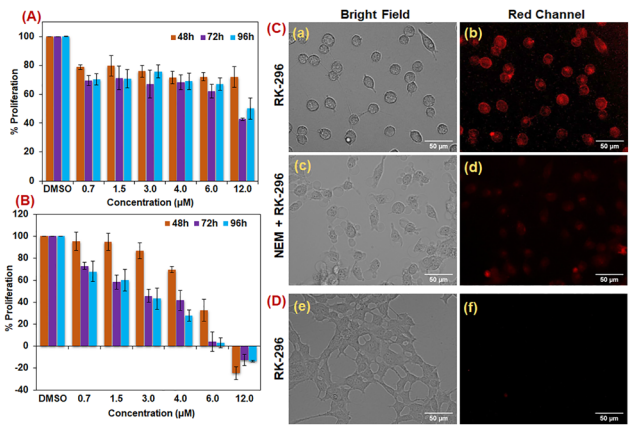

Fig. 20 Dose-dependent anti-proliferative activity of (A) **RK-296** and (B) NBDHEX in MDA-MB-231 cells. Fluorescence microscopy images (bright field and red channel) of (C) HeLa cells treated with **RK-296** (4 μM) alone (a–b) and pre-treated with NEM followed by **RK-296** (c–d), and (D) HEK-293 cells treated with **RK-296** alone (e–f), confirming the cellular incorporation of **RK-296** and the release of NIR fluorophore Biot-NIR-OH. HeLa cells were pre-treated with NEM to quench the endogenous thiols. Scale bar: 50 μm.

The importance of the biotin-moiety in **RK-296** in targeting cancer cells over normal cells was validated by the lack of fluorescence emission in the biotin receptor-negative HEK-293 cells (Fig. 20D). Taken together, these findings underscore the potential of a stimuli-responsive, turn-on fluorogenic prodrug strategy, in which sustained release of NBDHEX with real time imaging would be useful for alleviating its off-target side effects. While a partial release of NBDHEX could be achieved from **RK-296**, further research on an advanced prodrug strategy is needed for efficient release of NBDHEX from its prodrug with improved anticancer activity.

In addition, numerous studies have reported the multimodal anticancer activity of piperlongumine; however, its clinical application is constrained by poor pharmacokinetic properties.[97,98] Therefore, researchers have focused on designing several derivatives of piperlongumine,[99] as well as its prodrugs,[100] to enhance its therapeutic activity. Altogether, these reports indicate an urgent need to develop better GST inhibitors with enhanced pharmacokinetics and anticancer potency to mitigate cancer progression, as well as to implement combined prodrug strategies with chemotherapeutic drugs to overcome GST-related chemoresistance.

6. Future perspectives

Over the past decade, researchers have devoted considerable efforts towards the development of various stimuli-responsive, turn-on fluorogenic prodrugs that enable real-time bioimaging and fluorescence-associated precise and non-invasive monitoring for targeted drug delivery. The strategy offers additional benefits in reducing the drug-induced off-target toxicity to healthy cells. Numerous studies have explored the potential of fluorogenic prodrug strategies of selective inhibitors targeting key metabolic enzymes involved in glucose metabolism, nucleotide synthesis, DNA metabolism, and drug metabolism. In this review, these strategies are critically evaluated with particular emphasis on their respective therapeutic advantages and inherent limitations. Notably, stimuli-responsive dual-locked fluorogenic prodrug platforms have emerged as particularly promising candidates, offering enhanced therapeutic efficacy and reduced dose-limiting toxicity through improved control over site-specific drug activation. Despite the well-established advantages of prodrugs over conventional chemotherapeutics, systematic investigation of their pharmacological properties remains imperative for expediting successful clinical translation.

After careful analysis of the published literature, we learned that fine tuning of prodrug structures could significantly improve the pharmacokinetic properties of these systems, alongside improving the therapeutic efficacy required for clinical applications. For example, Mishra and co-workers reported an amphiphilic, GSH-sensitive, non-targeting prodrug of Dox and EPR, named **Dox/EPR-SS-TPGS**, as well as a cancer-cell targeting prodrug, **Dox/EPR-SS-TPGS-B6**.[37] They demonstrated that these amphiphilic micellar prodrugs increased the average

half-life of EPR and Dox by 2.87 and 3.37-fold, respectively, compared to free EPR + Dox. Notably, the half-life of EPR was extended from 3.5 h to 9 h in **EPR-SS-TPGS**, in which EPR is conjugated to d-α-tocopheryl polyethylene glycol succinate *via* a disulfide linker. These findings highlight the importance of structural modifications of enzyme inhibitor delivery systems to enhance plasma circulation time while enabling site-specific drug activation. Furthermore, the authors emphasized the critical role of cancer cell-targeting moieties, like vitamin B6, in the **Dox/EPR-SS-TPGS-B6** prodrug for enhanced cellular uptake and targeting properties. Similarly, our group highlighted the role of biotin receptor-mediated targeting in improving the selective uptake of the GSH-triggered NBDHEX prodrug (**RK-296**) in cancer cells over normal cells.[95] Collectively, these studies demonstrated that receptor-mediated targeting strategies can offer cancer cells selectivity to prodrugs, revealing an important approach towards the rational remodelling of enzyme inhibitors. Therefore, the strategic design of a prodrug system incorporating amphiphilic and cancer-cell-targeting moieties would represent a promising approach to improve pharmacokinetics and therapeutic applications.

In addition, increasing attention has been paid to the optimization of self-immolative linkers and stimuli-responsive moieties for precise tumour-site specific activation. For instance, our group reported distinct EPR release behaviour and cytotoxicity profiles for **RM-13** and **RM-28**, attributable to the presence of different esterase-responsive moieties, such as pivaloyloxymethyl ester in **RM-13** and a pivalate ester in **RM-28**.[38] Similarly, Yin and co-workers observed superior cytotoxicity of the boronic acid-containing prodrug **PBA-AMF** compared with the corresponding boronate ester analogue **PBE-AMF**, which was attributed to enhanced sialic acid-mediated cellular uptake.[77] Lee and co-workers further reported that the release profiles of amonafide prodrugs (**Amo-c-NO_2**, **Amo-NO_2**, **Amo-c-N_3**, **Amo-N_3** and **Amo-M**) are strongly influenced by both linker groups and triggering units.[80] Notably, the prodrugs in which amonafide was connected to the stimuli-responsive unit *via* a carbamate bond (**Amo-c-NO_2** and **Amo-c-N_3**) exhibited more efficient drug release than those directly conjugated through a C-N bond. Moreover, enhanced substrate specificity was observed for the enzyme (NTR)-triggered prodrug **Amo-c-NO_2** compared with the bioanalyte (H_2S)-responsive prodrug, **Amo-c-N_3**. In line with these findings, Qian and co-workers highlighted the advantages of the double-locked enzyme (HDAC and CTSL)-triggered prodrug (**AcKLP**) over the cysteine-triggered amonafide prodrug (**PhTLP**) in achieving selective inhibition of cancer cells over normal cells.[78] Similar linker-dependent effects have also been observed by our group for the **5-FU** prodrugs, such as **BJ-92** and **BJ-50**.[57] Our study revealed that the drug connected directly by a C-N bond in **BJ-50** was not cleavable by the self-immolative process. Given that only a handful of researchers have systematically evaluated the role of the linker and stimuli-responsive unit design in prodrug systems, detailed investigation into the rational optimization of suitable linker groups and activation mechanisms are essential for the development of advanced prodrug delivery systems.

As mentioned earlier, the development of chemoresistance remains a major limitation of conventional chemotherapy and is often associated with the overexpression of specific drug-metabolizing enzymes. Notable examples include the AR-mediated detoxification of doxorubicin and GSTP1-driven inactivation of cisplatin. To overcome these resistance mechanisms, several studies have explored the co-delivery strategies that combine chemotherapeutic drugs with the inhibitors of these metabolizing enzymes. For instance, Dox has been co-delivered with aldose reductase inhibitor EPR in the **Dox/EPR-SS-TPGS-B6** micellar prodrug system, resulting in better therapeutic outcomes.[37] Similarly, mutual prodrugs of cisplatin and its derivatives with the GSTP1 inhibitor NBDHEX have exhibited enhanced therapeutic efficacy against cisplatin-resistant cancer cell lines.[16] In addition, emerging evidence has indicated that the co-delivery of chemotherapeutic agents with gasotransmitter H_2S can mitigate dose-limiting toxicities towards healthy cells. For example, amonafide-H_2S releasing prodrugs (**AM-ITC** and **AM-TCB**), synthesized by our group, exhibited a significant reduction in amonafide-mediated toxicity in normal cells (HDF and HEK-293), which was attributed to the cytoprotective effects of H_2S.[74,76] Taken together, these findings highlight the potential of co-delivery strategies, either combining multiple therapeutic agents or pairing an anticancer agent with a cytoprotective gasotransmitter, to enhance therapeutic efficacy, while simultaneously minimizing off-target toxicity and the emergence of chemoresistance. Therefore, the rational design of prodrug systems with optimized pharmacokinetics, appropriate triggering moieties, and highly selective activation is important for enabling the clinical translation of multifunctional prodrug platforms.

7. Conclusions

This review illustrates the critical roles of key metabolic enzymes involved in glucose metabolism (aldose reductase), nucleotide synthesis (thymidylate synthase), DNA replication (Topoisomerases) and drug metabolism (glutathione-*S*-transferases) in cancer cell proliferation and the development of chemoresistance. Although several inhibitors targeting these enzymes are being explored for their anticancer potential, their clinical applications are constrained by suboptimal pharmacokinetic properties. Therefore, the transformative potential of stimuli-responsive prodrug systems for the targeted delivery of inhibitors against these enzymes has attracted substantial research attention, owing to their ability to enhance site-specific activation, improve bioavailability and reduce the off-target side effects. In particular, the stimuli-responsive, dual-locked, fluorogenic prodrugs offer the added advantage of precise and efficient delivery, facilitating real-time monitoring of active payload release while minimizing dose-limiting toxicity in normal cells. Beyond monotherapy, combination strategies integrating these enzyme inhibitors either with known FDA-approved chemotherapeutic drugs or with cytoprotective gasotransmitters have shown significant improvements in anticancer efficacy, exhibiting synergistic effects in both *in vitro*

and *in vivo* conditions with reduced off-target side effects and leading to prominent tumour growth inhibition. With the progressive trend in this field, we anticipate that the clinical translation of active enzyme inhibitors caged within stimuli-triggered delivery systems will represent a promising approach towards more effective and safer cancer treatments. Nevertheless, comprehensive investigations for their pharmacodynamics and safe pharmacology profiles remain essential to facilitate successful clinical application.

Author contributions

P. B., N. P., and R. K. contributed to writing the original draft of the manuscript. N. P. and R. K. contributed to writing the sections on reported prodrugs of enzyme inhibitors and the associated schematics. P. B. revised the draft further and modified the schematics and added other sections of the manuscript. K. P. B. wrote the original draft, edited, reviewed, and revised. K. P. B. corrected the figures/schemes, modified the draft, and prepared the final version. All authors have approved the final version of the manuscript.

Conflicts of interest

There are no conflicts to declare.

Data availability

No primary research results, software, or code have been included, and no new data were generated or analysed as part of this feature article.

Acknowledgements

K. P. B. acknowledges SERB (Reference No. CRG/2022/001158 and EEQ/2022/000071) for the research grants. We acknowledge DST-FIST (2017), CoE-FAST (2015), and the Department of Chemistry, CIF, NECBH (ref: BT/NER/143/SP44675/2023), and IIT Guwahati for providing infrastructural facilities. P. B. thanks CSIR, N. P. thanks PMRF and R. K. thanks IIT Guwahati for their fellowships.

Notes and references

1 D. Hanahan and Robert A. Weinberg, *Cell*, 2011, **144**, 646–674.
2 S. Nong, X. Han, Y. Xiang, Y. Qian, Y. Wei, T. Zhang, K. Tian, K. Shen, J. Yang and X. Ma, *MedComm*, 2023, **4**, e218.
3 M. Tufail, C.-H. Jiang and N. Li, *Mol. Cancer*, 2024, **23**, 203.
4 R. Li, S. Mei, Q. Ding, Q. Wang, L. Yu and F. Zi, *Sci. Rep.*, 2022, **12**, 18807.
5 P. Miao, S. Sheng, X. Sun, J. Liu and G. Huang, *IUBMB Life*, 2013, **65**, 904–910.
6 M. A. Khan, H. Zubair, S. Anand, S. K. Srivastava, S. Singh and A. P. Singh, *Cancer Lett.*, 2020, **473**, 176–185.
7 A. Schwab, A. Siddiqui, M. E. Vazakidou, F. Napoli, M. Böttcher, B. Menchicchi, U. Raza, Ö. Saatci, A. M. Krebs, F. Ferrazzi, I. Rapa, K. Dettmer-Wilde, M. J. Waldner, A. B. Ekici, S. A. K. Rasheed, D. Mougiakakos, P. J. Oefner, O. Sahin, M. Volante, F. R. Greten, T. Brabletz and P. Ceppi, *Cancer Res.*, 2018, **78**, 1604–1618.
8 A. Schwab, M. A. Siddiqui, V. Ramesh, P. N. Gollavilli, A. M. Turtos, S. S. Møller, L. Pinna, J. F. Havelund, A. M. A. Rømer, P. G. Ersan, B. Parma, S. Marschall, K. Dettmer, M. Alhusayan, P. Bertoglio, G. Querzoli, D. Mielenz, O. Sahin, N. J. Færgeman, I. A. Asangani and P. Ceppi, *Cell Death Differ.*, 2025, **32**, 587–597.
9 J. Chen, L. Cui, S. Lu and S. Xu, *Cell Death Dis.*, 2024, **15**, 42.
10 X. Liu, B. Ren, J. Ren, M. Gu, L. You and Y. Zhao, *Cell Commun. Sign.*, 2024, **22**, 380.
11 N. J. Mullen and P. K. Singh, *Nat. Rev. Cancer*, 2023, **23**, 275–294.
12 Ž. Skok, N. Zidar, D. Kikelj and J. Ilaš, *J. Med. Chem.*, 2020, **63**, 884–904.
13 Z.-N. Lei, Q. Tian, Q.-X. Teng, J. N. D. Wurpel, L. Zeng, Y. Pan and Z.-S. Chen, *MedComm*, 2023, **4**, e265.
14 S. Pathania, R. Bhatia, A. Baldi, R. Singh and R. K. Rawal, *Biomed. Pharmacother.*, 2018, **105**, 53–65.
15 D. M. Townsend and K. D. Tew, *Oncogene*, 2003, **22**, 7369–7375.
16 H. Chen, X. Wang and S. Gou, *J. Inorg. Biochem.*, 2019, **193**, 133–142.
17 F. Chen, X. Wen, S. Li, J. Wu, Y. Luo, Y. Gao, X. Yu and L. Chen, *Transl. Oncol.*, 2025, **55**, 102350.
18 A. Sen and D. Karati, *Naunyn Schmiedebergs Arch. Pharmacol.*, 2024, **397**, 5437–5448.
19 A. Acharya, N. Roy, V. Newaskar, A. Rai, A. Ghosh, M. Nagpure, S. K. Giri, G. Sahni and S. K. Guchhait, *Eur. J. Med. Chem.*, 2025, **291**, 117611.
20 H.-H. Han, H.-M. Wang, P. Jangili, M. Li, L. Wu, Y. Zang, A. C. Sedgwick, J. Li, X.-P. He, T. D. James and J. S. Kim, *Chem. Soc. Rev.*, 2023, **52**, 879–920.
21 M. H. Lee, A. Sharma, M. J. Chang, J. Lee, S. Son, J. L. Sessler, C. Kang and J. S. Kim, *Chem. Soc. Rev.*, 2018, **47**, 28–52.
22 S. Ma, J. H. Kim, W. Chen, L. Li, J. Lee, J. Xue, Y. Liu, G. Chen, B. Tang, W. Tao and J. S. Kim, *Adv. Sci.*, 2023, **10**, 2207768.
23 I.-C. Sun, H. Y. Yoon, D.-K. Lim and K. Kim, *Bioconjugate Chem.*, 2020, **31**, 1012–1024.
24 H. Martin, L. R. Lázaro, T. Gunnlaugsson and E. M. Scanlan, *Chem. Soc. Rev.*, 2022, **51**, 9694–9716.
25 J. Zeng, M. Liu, S. Li, D. Cheng, L. He and L. Yuan, *ChemBioChem*, 2023, **24**, e202300035.
26 Y. Tu, J. Gong, J. Mou, H. Jiang, H. Zhao and J. Gao, *Front. Pharmacol.*, 2024, **15**, 1434137.
27 R. Tammali, S. K. Srivastava and K. V. Ramana, *Curr. Cancer Drug Targets*, 2011, **11**, 560–571.
28 T. Matsunaga, Y. Wada, S. Endo, M. Soda, O. El-kabbani and A. Hara, *Front. Pharmacol.*, 2012, **3**, 1–11.
29 N. P. Syamprasad, S. Jain, B. Rajdev, N. Prasad, R. Kallipalli and V. G. M. Naidu, *Biochem. Pharmacol.*, 2023, **211**, 115528.
30 K. G. de la Cruz-López, L. J. Castro-Muñoz, D. O. Reyes-Hernández, A. García-Carrancá and J. Manzo-Merino, *Front. Oncol.*, 2019, **9**, 1143.
31 H. Sonowal, P. B. Pal, J.-J. Wen, S. Awasthi, K. V. Ramana and S. K. Srivastava, *Sci. Rep.*, 2017, **7**, 3182.
32 T. M. Penning, S. Jonnalagadda, P. C. Trippier and T. L. Rižner, *Pharmacol. Rev.*, 2021, **73**, 1150–1171.
33 L. Quattrini and C. La Motta, *Expert Opin. Ther. Pat.*, 2019, **29**, 199–213.
34 N. Hotta, Y. Akanuma, R. Kawamori, K. Matsuoka, Y. Oka, M. Shichiri, T. Toyota, M. Nakashima, I. Yoshimura, N. Sakamoto and Y. Shigeta, *Diabetes Care*, 2006, **29**, 1538–1544.
35 C. Bailly, *Eur. J. Pharmacol.*, 2022, **931**, 175191.
36 L. Zhang, H. Zhang, Y. Zhao, Z. Li, S. Chen, J. Zhai, Y. Chen, W. Xie, Z. Wang, Q. Li, X. Zheng and X. Hu, *FEBS Lett.*, 2013, **587**, 3681–3686.
37 V. T. Banala, S. Urandur, S. Sharma, M. Sharma, R. P. Shukla, D. Marwaha, S. Gautam, M. Dwivedi and P. R. Mishra, *Biomater. Sci.*, 2019, **7**, 2889–2906.
38 R. Misra, P. Barman and K. P. Bhabak, *ACS Appl. Bio Mater.*, 2024, **7**, 6542–6553.
39 J. Zhai, H. Zhang, L. Zhang, Y. Zhao, S. Chen, Y. Chen, X. Peng, Q. Li, M. Yuan and X. Hu, *ChemMedChem*, 2013, **8**, 1462–1464.
40 S. R. Cheekatla, *Chem.*, 2025, **7**, 118.
41 N. Touroutoglou and R. Pazdur, *Clin. Cancer Res.*, 1996, **2**, 227–243.
42 C. Burdelski, C. Strauss, M. C. Tsourlakis, M. Kluth, C. Hube-Magg, N. Melling, P. Lebok, S. Minner, C. Koop, M. Graefen, H. Heinzer,

C. Wittmer, T. Krech, G. Sauter, W. Wilczak, R. Simon, T. Schlomm and S. Steurer, *Oncotarget*, 2015, **6**, 8377–8387.
43 M. G. Rose, M. P. Farrell and J. C. Schmitz, *Clin. Colorectal Cancer*, 2002, **1**, 220–229.
44 C. Heidelberger, N. K. Chaudhuri, P. Danneberg, D. Mooren, L. Griesbach, R. Duschinsky, R. J. Schnitzer, E. Pleven and J. Scheiner, *Nature*, 1957, **179**, 663–666.
45 M. Malet-Martino, P. Jolimaitre and R. Martino, *Curr. Med. Chem. Anticancer Agents*, 2002, **2**, 267–310.
46 V. Ciaffaglione, M. N. Modica, V. Pittalà, G. Romeo, L. Salerno and S. Intagliata, *ChemMedChem*, 2021, **16**, 3496–3512.
47 S. Sarkar, S. Kiren and W. H. Gmeiner, *Pharmaceutics*, 2024, **16**, 734.
48 X. Zhang, X. Li, Z. Li, X. Wu, Y. Wu, Q. You and X. Zhang, *Org. Lett.*, 2018, **20**, 3635–3638.
49 Y. Ai, O. N. Obianom, M. Kuser, Y. Li, Y. Shu and F. Xue, *ACS Med. Chem. Lett.*, 2019, **10**, 127–131.
50 R. Kumar, J. Han, H.-J. Lim, W. X. Ren, J.-Y. Lim, J.-H. Kim and J. S. Kim, *J. Am. Chem. Soc.*, 2014, **136**, 17836–17843.
51 W. Liu, H. Liu, X. Peng, G. Zhou, D. Liu, S. Li, J. Zhang and S. Wang, *Bioconjugate Chem.*, 2018, **29**, 3332–3343.
52 W. H. Gmeiner, *Molecules*, 2020, **25**, 3438.
53 B. Perillo, M. Di Donato, A. Pezone, E. Di Zazzo, P. Giovannelli, G. Galasso, G. Castoria and A. Migliaccio, *Exp. Mol. Med.*, 2020, **52**, 192–203.
54 W.-X. Wang, W.-L. Jiang, G.-J. Mao, Z.-K. Tan, M. Tan and C.-Y. Li, *Chem. Commun.*, 2021, **57**, 13768–13771.
55 T. Jiang, Q. Zeng and J. He, *Transl. Cancer Res.*, 2023, **12**, 2932–2945.
56 K. Tyagi, R. Kumari and V. Venkatesh, *Org. Biomol. Chem.*, 2023, **21**, 4455–4464.
57 M. Badirujjaman, R. P. Thummer and K. P. Bhabak, *Chem. – Asian J.*, 2025, **20**, e202400846.
58 T. Ubhi and G. W. Brown, *Cancer Res.*, 2019, **79**, 1730–1739.
59 C. O. Okoro and T. H. Fatoki, *Int. J. Mol. Sci.*, 2023, **24**, 2532.
60 J. L. Nitiss, *Nat. Rev. Cancer*, 2009, **9**, 327–337.
61 J. L. Nitiss, *Nat. Rev. Cancer*, 2009, **9**, 338–350.
62 X. An, F. Xu, R. Luo, Q. Zheng, J. Lu, Y. Yang, T. Qin, Z. Yuan, Y. Shi, W. Jiang and S. Wang, *BMC Cancer*, 2018, **18**, 331.
63 X. Cheng, Y. Wei, L. Deng, H. Dong, H. Wei, C. Xie, Y. Tuo, M. Chen, H. Qin and Y. Cao, *Discov. Oncol.*, 2024, **15**, 423.
64 R. Rezonja, L. Knez, T. Cufer and A. Mrhar, *Radiol. Oncol.*, 2013, **47**, 1–13.
65 C. Belger, C. Abrahams, A. Imamdin and S. Lecour, *IJC Heart Vasc.*, 2024, **50**, 101332.
66 A. Sharma, E.-J. Kim, H. Shi, J. Y. Lee, B. G. Chung and J. S. Kim, *Biomaterials*, 2018, **155**, 145–151.
67 C. Skarbek, S. Serra, H. Maslah, E. Rascol and R. Labruère, *Bioorg. Chem.*, 2019, **91**, 103158.
68 O. O. Krasnovskaya, V. M. Malinnikov, N. S. Dashkova, V. M. Gerasimov, I. V. Grishina, I. I. Kireev, S. V. Lavrushkina, P. A. Panchenko, M. A. Zakharko, P. A. Ignatov, O. A. Fedorova, G. Jonusauskas, D. A. Skvortsov, S. S. Kovalev, E. K. Beloglazkina, N. V. Zyk and A. G. Majouga, *Bioconjugate Chem.*, 2019, **30**, 741–750.
69 Y. Liu, S. Corrales-Guerrero, J. C. Kuo, R. Robb, G. Nagy, T. Cui, R. J. Lee and T. M. Williams, *ACS Omega*, 2024, **9**, 977–987.
70 C. Ge, X. Di, S. Han, M. Wang, X. Qian, Z. Su, H.-K. Liu and Y. Qian, *Chem. Commun.*, 2021, **57**, 1931–1934.
71 A. Sufian, D. Bhattacherjee, P. Barman, R. Kesarwani, S. Das and K. P. Bhabak, *Chem. Commun.*, 2025, **61**, 4647–4661.
72 E. Calatrava-Pérez, L. A. Marchetti, G. J. McManus, D. M. Lynch, R. B. P. Elmes, D. C. Williams, T. Gunnlaugsson and E. M. Scanlan, *Chem. – Eur. J.*, 2022, **28**, e202103858.
73 O. Kabil, N. Motl and R. Banerjee, *Biochim. Biophys. Acta, Proteins Proteomics*, 2014, **1844**, 1355–1366.
74 S. K. Mahato, P. Barman, M. Badirujjaman and K. P. Bhabak, *Chem. Commun.*, 2023, **59**, 4802–4805.
75 S. Du, Y. Huang, H. Jin and T. Wang, *Front. Pharmacol.*, 2018, **9**, 32.
76 A. Sufian, M. Badirujjaman, P. Barman and K. P. Bhabak, *Chem. – Eur. J.*, 2023, **29**, e202302197.
77 X. Yao, W. Sun, Y. Yuan, J. Hu, J. Fu and J. Yin, *Bioorg. Chem.*, 2024, **150**, 107560.
78 W. Cheng, Y. Yang, B. Zhang, C.-W. Shao, W. Chen, R. Xia, W. Sun, X. Zhao, B. Zhang, X. Luo, T. D. James and Y. Qian, *Chem. Sci.*, 2024, **15**, 19336–19344.
79 Z. Chen, F. Han, Y. Du, H. Shi and W. Zhou, *Signal Transduction Targeted Ther.*, 2023, **8**, 70.
80 S. A. Yoon, J. Roh, J. Kil, S.-K. Ko and M. H. Lee, *Sens. Actuators, B*, 2026, **447**, 138911.
81 E. Laborde, *Cell Death Differ.*, 2010, **17**, 1373–1380.
82 R. R. Singh and K. M. Reindl, *Antioxidants*, 2021, **10**, 701.
83 S. M. Alnasser, *Genes Dis.*, 2025, **12**, 101482.
84 S. Singh, *Cancer Chemother. Pharmacol.*, 2015, **75**, 1–15.
85 N. Allocati, M. Masulli, C. Di Ilio and L. Federici, *Oncogenesis*, 2018, **7**, 8.
86 T. Wang, P. Arifoglu, Z. E. Ronai and K. D. Tew, *J. Biol. Chem.*, 2001, **276**, 20999–21003.
87 N. Lv, C. Huang, H. Huang, Z. Dong, X. Chen, C. Lu and Y. Zhang, *Antioxidants*, 2023, **12**, 1970.
88 B. O. Al-Najjar, M. Helal, F. G. Saqallah and B. Bandy, *RSC Med. Chem.*, 2025, **16**, 1516–1531.
89 W. Harshbarger, S. Gondi, S. B. Ficarro, J. Hunter, D. Udayakumar, D. Gurbani, W. D. Singer, Y. Liu, L. Li, J. A. Marto and K. D. Westover, *J. Biol. Chem.*, 2017, **292**, 112–120.
90 H. Sha, S. Dong, C. Yu, R. Zou, Y. Zhu, Y. Lu, J. Zhang, H. Cao, D. Chen, J. Wu and J. Feng, *J. Cancer*, 2020, **11**, 7216–7223.
91 H. Sha, R. Zou, Y. Lu, Y. Gan, R. Ma, J. Feng and D. Chen, *Cancer Med.*, 2023, **12**, 5833–5845.
92 D. Rotili, A. De Luca, D. Tarantino, S. Pezzola, M. Forgione, B. Morozzo della Rocca, M. Falconi, A. Mai and A. M. Caccuri, *Eur. J. Med. Chem.*, 2015, **89**, 156–171.
93 Y. Chen, W. Pan, X. Ding, L. Zhang, Q. Xia, Q. Wang, Q. Chen, Q. Gao, J. Yan, R. Lesyk, Z. Tang and X. Han, *Tetrahedron*, 2023, **138**, 133393.
94 Q. Liu, Z. Liu, W. Hua and S. Gou, *J. Med. Chem.*, 2021, **64**, 1701–1712.
95 R. Kesarwani, N. Pal and K. P. Bhabak, *Chem. Commun.*, 2024, **60**, 3397–3400.
96 N. Roy and P. Paira, *ACS Omega*, 2024, **9**, 20670–20701.
97 D. Parama, V. Rana, S. Girisa, E. Verma, U. D. Daimary, K. K. Thakur, A. Kumar and A. B. Kunnumakkara, *Explor. Target. Anti-tumor Ther.*, 2021, **2**, 323–354.
98 S. Mitra, P. Biswas, A. Bandyopadhyay, V. S. Gadekar, A. V. Gopalakrishnan, M. Kumar, Radha and S. Nandy, *Naunyn Schmiedebergs Arch. Pharmacol.*, 2024, **397**, 2637–2650.
99 S. S. Swain and S. K. Sahoo, *Arch. Pharm.*, 2024, **357**, 2300768.
100 Y. Zou, X. Wan, Z. Ding, C. Tang, C. Wang and X. Chen, *Fitoterapia*, 2024, **177**, 106091.